

Finite Element Representations of Gaussian Processes: Balancing Numerical and Statistical Accuracy

Daniel Sanz-Alonso and Ruiyi Yang

University of Chicago

Abstract

The stochastic partial differential equation approach to Gaussian processes (GPs) represents Matérn GP priors in terms of n finite element basis functions and Gaussian coefficients with sparse precision matrix. Such representations enhance the scalability of GP regression and classification to datasets of large size N by setting $n \approx N$ and exploiting sparsity. In this paper we reconsider the standard choice $n \approx N$ through an analysis of the estimation performance. Our theory implies that, under certain smoothness assumptions, one can reduce the computation and memory cost without hindering the estimation accuracy by setting $n \ll N$ in the large N asymptotics. Numerical experiments illustrate the applicability of our theory and the effect of the prior lengthscale in the pre-asymptotic regime.

1 Introduction

Gaussian processes (GPs) are an important model for prior distributions over functions, and play a central role in spatial statistics, machine learning, Bayesian inverse problems, and a variety of other scientific and engineering applications [44, 56, 48, 49, 33, 32]. However, GP methodology often suffers from the *big N problem*: conditioning a GP to N observations requires to factorize an $N \times N$ covariance matrix, with a general cost of $O(N^3)$. Numerous approaches to address this challenge have been developed [22]. The aim of this paper is to provide novel understanding of the popular stochastic partial differential equation (SPDE) approach [28, 29] for GP regression and classification with large datasets.

Let $u(\mathbf{x})$ be a Matérn-type GP (see e.g. [3] or Subsection 2.1 below) on a bounded domain $\mathcal{D} \subset \mathbb{R}^D$. The SPDE approach approximates u with a GP u_h of the form

$$u_h(\mathbf{x}) = \sum_{i=1}^{n_h} w_i e_i(\mathbf{x}), \quad \mathbf{x} \in \mathcal{D}, \quad (1.1)$$

where $e_i : \mathcal{D} \rightarrow \mathbb{R}$ are finite element (FE) basis functions and $\mathbf{w} := (w_1, \dots, w_{n_h})^\top \sim \mathcal{N}(\mathbf{0}, \mathbf{Q}^{-1})$ with sparse precision matrix $\mathbf{Q} \in \mathbb{R}^{n_h \times n_h}$. The dimension n_h of the basis $\{e_i\}_{i=1}^{n_h}$ is determined by a mesh-size parameter $h > 0$. Previous work sets h so that $n_h \approx N$, and the $O(N^3)$ computational cost is reduced by exploiting the local support of the FE basis functions e_i and the sparsity of \mathbf{Q} , see e.g. [28, 2, 1] or Subsection 2.3. However, the choice $n_h \approx N$ has not been theoretically or empirically investigated. In particular, it is not clear if the computational gain achieved with $n_h \approx N$ comes at the price of larger estimation error. In this paper we shall introduce a framework for selecting n_h based on the posterior estimation performance achieved when using GP prior u_h . Our theory implies that, under certain smoothness assumptions, choosing $n_h \ll N$ can indeed be sufficient in the large N asymptotics, as otherwise the statistical errors inherent to the regression or classification tasks dominate the numerical error in the approximation $u_h \approx u$. Therefore, in

addition to the computational gain facilitated by sparsity, there is a second computational and memory gain: the *dimension* of the matrices that need to be factorized can be reduced in large N regimes without hindering the estimation accuracy. Numerical experiments will illustrate the applicability of our theory and the effect of the prior lengthscale in the pre-asymptotic regime.

The SPDE approach is part of a trend in GP methodology that seeks to leverage sparsity for computational efficiency [34]. In this spirit, one can construct sparse approximations of the covariance matrix of the observations (a procedure known as *tapering* or *localization* [16, 14]), or of the precision matrix [9] and its Cholesky factor [39, 24]. Other approaches exploiting sparsity include Vecchia approximations [53, 25] and methods based on the screening effect [46]. These techniques are well established in several applications and are essential, for example, in the practical implementation of data assimilation algorithms for numerical weather forecasting [23]. A complementary line of work relies on *smoothness* rather than sparsity for computational expediency. For instance, truncated Karhunen-Loève expansions in Bayesian inverse problems rely on a representation of the form (1.1) with small dimension n , spectral basis functions, and stochastic weights with diagonal covariance [48]. These low-rank representations [40, 20] have been claimed to remove fine-scale variations of the process [1], but can be accurate if the underlying process is smooth. Our work blends sparsity and smoothness demonstrating that, for regression and classification with large data-sets, sparse methods can benefit from a significant dimension reduction under mild smoothness assumptions.

To propose a criterion for choosing n_h with respect to N , we will exploit the concept of posterior contraction rates [18], which is discussed in Subsection 2.4. Roughly speaking, we consider a scaling sufficient if the posterior constructed with GP prior u_h contracts at the same rate as the posterior constructed with the true GP prior u . The Bayesian nonparametrics framework in [50] guarantees that if the rate of convergence of the GP prior approximation $u_h \approx u$ is fast enough, then the corresponding posteriors contract at the same rate. Establishing convergence rates for approximations $u_h \approx u$ is an active research area on numerical analysis of FE solution of fractional SPDEs [3, 1, 7]. As part of our analysis, we derive a crude estimate of the approximation error $\mathbb{E}\|u_h - u\|_\infty^2$ for a particular FE discretization when \mathcal{D} is a hyperrectangle. The result holds for general dimension D while being less sharp than the one-dimensional result in [7], which also allows for more general domains. However, our main objective is to illustrate that the plug-in character of the framework [50] allows to seamlessly translate L^∞ and L^2 error bounds for the approximation $u_h \approx u$ into sufficient choices of n_h in terms of N in regression and classification settings. As we shall see, even crude error bounds suggest that, in the large N asymptotics, $n_h \ll N$ can be sufficient under mild smoothness assumptions.

Numerical simulations in the regression setting will complement our theoretical analysis. Our experiments illustrate that (i) the qualitative theoretical behavior suggested by our large N asymptotic analysis is in agreement with the behavior observed with moderate sample-size; (ii) if the truth is not smooth and has a short lengthscale, choosing $n_h \gg N$ may indeed be necessary for the SPDE approach to match the estimation accuracy of the ground truth prior model; and (iii) outside the large N asymptotic regime, the prior lengthscale plays an important role in determining appropriate choice of n_h in terms of N . This last point is also partly explained by our theory, where the lengthscale appears as a prefactor in the error bound for the FE prior representations. We believe these findings together with our theoretical results provide useful insights for calibrating the FE approach in practice.

The study of fixed-domain, large N asymptotics [44, 42, 41, 45, 11, 54] is motivated by applications

in environmental science, ecology, climate, and hydrology, where N is often in the order of hundreds of thousands or larger. At a high level, our criterion resembles the in-fill asymptotic analysis of tapered covariance functions in [14], where the authors give conditions on the taper function that guarantee large-data asymptotic equivalence of the mean-squared prediction error of the true and tapered covariance models. As in [14], we may interpret u_h as defining a misspecified covariance model and then, similar to [14, 43], our criterion guarantees that the misspecification is inconsequential in a large-data regime. On the other hand, even if the Matérn-type GP u is not interpreted as a ground truth prior model, our analysis suggests that over-discretizing the FE representations u_h should be avoided, as there is a threshold beyond which further discretizing increases the computational cost without improving the estimation accuracy. Similar ideas permeate the study of the value of unlabeled data in semi-supervised learning [37] with graph representations of Matérn GPs [36].

The rest of this paper is organized as follows. We provide all necessary background and formalize our problem setting in Section 2. Our main results are in Section 3 and complementary numerical experiments in Section 4. We close in Section 5 with possible extensions of our main results and open directions that stem from our work. All the proofs are deferred to Section 6.

Notation. For a, b two real numbers, we denote $a \wedge b = \min\{a, b\}$ and $a \vee b = \max\{a, b\}$. The symbol \lesssim will denote less than or equal to up to a universal constant. For two real sequences $\{a_i\}$ and $\{b_i\}$, we denote (i) $a_i \ll b_i$ if $\lim_i(a_i/b_i) = 0$; (ii) $a_i = O(b_i)$ if $\limsup_i(a_i/b_i) \leq C$ for some positive constant C ; and (iii) $a_i \asymp b_i$ if $c_1 \leq \liminf_i(a_i/b_i) \leq \limsup_i(a_i/b_i) \leq c_2$ for some positive constants c_1, c_2 . For a nonnegative integer K , we denote $[K] = \{0, \dots, K\}$.

2 Background and Problem Setting

To make our presentation self-contained, we introduce in this section all necessary background and formalize our problem setting. Matérn-type GPs and their connection with the classical Matérn covariance function are discussed in Subsection 2.1. Subsection 2.2 reviews FE representations of Matérn-type GPs. Our regression and classification problem settings are formalized in Subsection 2.3, where we also summarize how FE representations of Matérn-type GPs allow to speed up computations. Finally, Subsection 2.4 overviews the Bayesian nonparametrics framework that we employ as our criterion to identify sufficient scalings of n_h with respect to N .

2.1 The Matérn Covariance Function and SPDE Representations

Recall that the Matérn covariance function is defined by

$$c_{\text{Mat}}(\mathbf{x}, \mathbf{x}') = \sigma^2 \frac{2^{1-\nu}}{\Gamma(\nu)} (\kappa |\mathbf{x} - \mathbf{x}'|)^\nu K_\nu(\kappa |\mathbf{x} - \mathbf{x}'|), \quad \mathbf{x}, \mathbf{x}' \in \mathbb{R}^D, \quad (2.1)$$

where $|\cdot|$ is the Euclidean distance on \mathbb{R}^D , Γ is the gamma function and K_ν is the modified Bessel function of the second kind. The parameters σ , ν , κ control, respectively, the marginal variance, smoothness of the sample paths, and correlation lengthscale. Due to its flexibility, the Matérn model is widely used in spatial statistics [44, 17], machine learning [56], and uncertainty quantification [49], with applications in various scientific fields [21, 4]. The connection between the Matérn covariance and SPDEs has long been noticed [55]. Consider formally the equation

$$(\kappa^2 - \Delta)^{s/2} u = \kappa^{s-D/2} \mathcal{W} \quad \text{in } \mathcal{D}, \quad (2.2)$$

where $s = \nu + D/2$, Δ is a Laplacian and \mathcal{W} is a spatial white noise. (Here and below we will ignore the marginal variance which acts only as a scaling factor.) If $\mathcal{D} := \mathbb{R}^D$, then the unique stationary solution to (2.2), suitably interpreted [55], has covariance function (2.1).

Following [28], we will define *Matérn-type GPs* by solution of (2.2) in a *bounded* domain $\mathcal{D} \subset \mathbb{R}^D$, interpreting the SPDE (2.2) as in [3]. We outline here the main ideas and refer to [3] for further details. Let $\mathcal{L} := \kappa^2 - \Delta$ be equipped with homogeneous Dirichlet or Neumann boundary condition. The eigenfunctions $\{\psi_i\}_{i=1}^\infty$ of the Dirichlet (or Neumann) Laplacian form an orthonormal basis of $L^2(\mathcal{D})$, where the associated ordered eigenvalues $\{\lambda_i\}_{i=1}^\infty$ satisfy $\lambda_i \asymp i^{2/D}$ by Weyl's law (see e.g. [10, Theorem 6.3.1]). The fractional power operator $\mathcal{L}^{s/2}$ in (2.2) is then defined by

$$\mathcal{L}^{s/2}u := \sum_{i=1}^{\infty} (\kappa^2 + \lambda_i)^{s/2} \langle u, \psi_i \rangle \psi_i$$

with domain $\{u \in L^2(\mathcal{D}) : \sum_{i=1}^{\infty} (\kappa^2 + \lambda_i)^s \langle u, \psi_i \rangle^2 < \infty\}$, where $\langle \cdot, \cdot \rangle$ denotes the $L^2(\mathcal{D})$ -inner product. The white noise in (2.2) is formally defined by the series $\mathcal{W} = \sum_{i=1}^{\infty} \xi_i \psi_i$, with $\xi_i \stackrel{i.i.d.}{\sim} \mathcal{N}(0, 1)$ set on a complete probability space $(\Omega, \mathcal{A}, \mathbb{P})$. As rigorously shown in [3, Lemma 2.1], existence and uniqueness of solutions to (2.2) in $L^2(\Omega; L^2(\mathcal{D}))$ is guaranteed for $s > D/2$. Moreover, the solution can be represented as a series expansion

$$u(\mathbf{x}) = \kappa^{s-D/2} \sum_{i=1}^{\infty} (\kappa^2 + \lambda_i)^{-s/2} \xi_i \psi_i(\mathbf{x}), \quad \xi_i \stackrel{i.i.d.}{\sim} \mathcal{N}(0, 1), \quad \mathbf{x} \in \mathcal{D}, \quad (2.3)$$

where the assumption $s > D/2$ together with Weyl's law guarantees that $u \in L^2(\mathcal{D})$ almost surely. We refer to u defined by (2.3) as a Matérn-type GP. The covariance function of Matérn-type GPs no longer agrees with the classical Matérn covariance model (2.1), but approximates it well away from the boundary —see for instance Proposition 3.1 below.

2.2 Finite Element Representations of Matérn-type Gaussian Processes

Let $\mathcal{D} \subset \mathbb{R}^D$ be a bounded domain and let $\{V_h\}_{h \in (0,1)}$ be a family of subspaces of $H^1(\mathcal{D})$ (the space of functions whose weak derivatives belong to $L^2(\mathcal{D})$) with finite dimensions $n_h := \dim(V_h) < \infty$. In subsequent developments h will play the role of a mesh-size parameter and $n_h \asymp h^{-D}$. Consider the Galerkin discretization $-\Delta_h : V_h \rightarrow V_h$ of $-\Delta$ defined as

$$\langle -\Delta_h u_h, v_h \rangle = \langle -\Delta u_h, v_h \rangle \quad \forall u_h, v_h \in V_h.$$

Let $\{(\lambda_{h,i}, \psi_{h,i})\}_{i=1}^{n_h}$ be the eigenpairs of $-\Delta_h$ satisfying

$$\langle -\Delta_h \psi_{h,i}, v_h \rangle = \lambda_{h,i} \langle \psi_{h,i}, v_h \rangle \quad \forall v_h \in V_h,$$

where we assume the $\lambda_{h,i}$'s are in increasing order and the $\psi_{h,i}$'s are orthonormal. We then define a discretization of the SPDE (2.2) by

$$\mathcal{L}_h^{s/2} u_h := (\kappa^2 - \Delta_h)^{s/2} u_h = \kappa^{s-D/2} \mathcal{W}_h, \quad \mathcal{W}_h := \sum_{i=1}^{n_h} \xi_i \psi_{h,i}, \quad \xi_i \stackrel{i.i.d.}{\sim} \mathcal{N}(0, 1). \quad (2.4)$$

We refer to the solution u_h as a FE representation of the Matérn-type GP u . Note that

$$u_h(\mathbf{x}) = \kappa^{s-D/2} \sum_{i=1}^{n_h} (\kappa^2 + \lambda_{h,i})^{-s/2} \xi_i \psi_{h,i}(\mathbf{x}), \quad \xi_i \stackrel{i.i.d.}{\sim} \mathcal{N}(0, 1), \quad \mathbf{x} \in \mathcal{D}. \quad (2.5)$$

Inspection of (2.3) and (2.5) suggests that the error in the approximation $u_h \approx u$ is largely determined by the FE error in the approximations $\lambda_{h,i} \approx \lambda_i$ and $\psi_{h,i} \approx \psi_i$. We will pursue this idea in our error analysis in Section 3. However, the Karhunen-Loève representation (2.5) is not in general useful for practical implementation, as the eigenpairs $\{(\lambda_{h,i}, \psi_{h,i})\}_{i=1}^{n_h}$ can be expensive to compute and the eigenfunctions do not have compact support. The following result from [28] shows that the solution to (2.4) admits an equivalent representation in terms of a FE basis, as foreshadowed in (1.1).

Proposition 2.1. *Let $\{e_{h,i}\}_{i=1}^{n_h}$ be a FE basis of V_h , and denote by \mathbf{M} and \mathbf{G} the mass and stiffness matrices with entries $\mathbf{M}_{ij} = \langle e_{h,i}, e_{h,j} \rangle$ and $\mathbf{G}_{ij} = \langle \nabla e_{h,i}, \nabla e_{h,j} \rangle$. For $0 \neq s \in \mathbb{N}$, the FE representation u_h of the Matérn-type GP u admits the characterization*

$$u_h(\mathbf{x}) = \sum_{i=1}^{n_h} w_i e_{h,i}(\mathbf{x}), \quad \mathbf{w} \sim \mathcal{N}(\mathbf{0}, \mathbf{Q}^{-1}), \quad (2.6)$$

where $\mathbf{Q} = (\kappa^2 \mathbf{M} + \mathbf{G})[\mathbf{M}^{-1}(\kappa^2 \mathbf{M} + \mathbf{G})]^{s-1}$.

Notice that (2.6) does not involve the eigenpairs. Moreover, the matrices \mathbf{M} and \mathbf{G} are sparse for standard FE basis $e_{h,i}$, e.g. tent functions. Lumping the mass matrix \mathbf{M} ensures sparsity of \mathbf{Q} and gives a Gauss-Markov approximation to the Matérn-type GP u [28]. For $s \notin \mathbb{N}$, the rational SPDE approach can be adopted [1].

2.3 Gaussian Process Regression and Classification: Finite Element Representations

Here we introduce the regression and classification models we consider, and describe briefly how FE representations of Matérn-type GPs can alleviate the computational burden of these tasks. Given N pairs of data $\{(\mathbf{X}_i, Y_i)\}_{i=1}^N$ we are interested in inferring $f_0(\mathbf{x}) = \mathbb{E}[Y|\mathbf{X} = \mathbf{x}]$ under the following data-generating mechanisms:

- Fixed design regression: $Y_i = f_0(\mathbf{X}_i) + \eta_i$, where the \mathbf{X}_i 's are fixed (and distinct) covariates and $\eta_i \stackrel{i.i.d.}{\sim} \mathcal{N}(0, \tau^2)$ with τ known.
- Binary classification: $\mathbb{P}(Y_i = 1|\mathbf{X}_i) = f_0(\mathbf{X}_i)$, where $\mathbf{X}_i \stackrel{i.i.d.}{\sim} \mu$ for some distribution μ over \mathcal{D} .

For simplicity we shall assume for the rest of this paper that μ is the uniform distribution over \mathcal{D} , but we note that it suffices to assume that μ admits a Lebesgue density bounded above and below by positive constants.

For fixed design regression, we set a FE Matérn-type GP prior u_h on f_0 . The posterior of the weights \mathbf{w} is given by

$$\mathbf{w} | \{(\mathbf{X}_i, Y_i)\}_{i=1}^N \sim \mathcal{N}((\mathbf{S}^\top \mathbf{S} + \tau^2 \mathbf{Q})^{-1} \mathbf{S}^\top \mathbf{y}, (\tau^{-2} \mathbf{S}^\top \mathbf{S} + \mathbf{Q})^{-1}),$$

where $\mathbf{S} \in \mathbb{R}^{N \times n_h}$ has entries $\mathbf{S}_{ij} = e_j(\mathbf{X}_i)$ and $\mathbf{y} = (Y_1, \dots, Y_N)^\top$. The main computational cost for posterior inference is in factorizing the $n_h \times n_h$ matrix $\mathbf{S}^\top \mathbf{S} + \tau^2 \mathbf{Q}$. This factorization can be

efficiently computed since the local support of standard FE basis functions ensures sparsity of \mathbf{S} , and \mathbf{Q} can be made sparse as discussed in Subsection 2.2.

For binary classification, let Φ be the logistic function and consider a wrapped GP prior $\Phi \circ u_h$ over f_0 . The posterior log-density is given by

$$\begin{aligned} \log \mathbb{P}(\mathbf{w} | \{(\mathbf{X}_i, Y_i)\}_{i=1}^N) &= \sum_{i=1}^N Y_i \log \Phi((\mathbf{S}\mathbf{w})_i) + (1 - Y_i) \log(1 - \Phi((\mathbf{S}\mathbf{w})_i)) \\ &\quad - \frac{1}{2} \mathbf{w}^\top \mathbf{Q} \mathbf{w} + \text{const}, \end{aligned} \quad (2.7)$$

where $(\mathbf{S}\mathbf{w})_i$ denotes the i -th entry of $\mathbf{S}\mathbf{w}$. Two standard procedures for posterior inference are *maximum a posteriori* (MAP) estimation and Markov chain Monte Carlo (MCMC) sampling. To compute the MAP estimate, (2.7) is optimized to recover the weights with highest posterior density. This optimization problem can be efficiently solved using the Hessian of the objective function, which takes the form $\mathbf{S}^\top \mathbf{D} \mathbf{S} - \mathbf{Q}$, where \mathbf{D} is a diagonal matrix with

$$\mathbf{D}_{ii} = \Phi''((\mathbf{S}\mathbf{w})_i) \left[\frac{Y_i}{\Phi((\mathbf{S}\mathbf{w})_i)} - \frac{1 - Y_i}{1 - \Phi((\mathbf{S}\mathbf{w})_i)} \right] - [\Phi'((\mathbf{S}\mathbf{w})_i)]^2 \left[\frac{Y_i}{\Phi((\mathbf{S}\mathbf{w})_i)^2} + \frac{1 - Y_i}{(1 - \Phi((\mathbf{S}\mathbf{w})_i))^2} \right].$$

Therefore, the computational cost is largely determined by the sparsity of the matrix $\mathbf{S}^\top \mathbf{D} \mathbf{S} - \mathbf{Q}$, which in turn depends on the sparsity of \mathbf{S} and \mathbf{Q} . On the other hand, MCMC algorithms for posterior inference with GP priors have been widely studied [30, 6, 8, 15, 38], and a key idea behind these methods is to employ a proposal mechanism $\mathbf{w} \mapsto \mathbf{w}'$ of the form

$$\mathbf{w}' = \theta \mathbf{w} + (1 - \theta)^{1/2} \boldsymbol{\gamma}, \quad \boldsymbol{\gamma} \sim \mathcal{N}(\mathbf{0}, \mathbf{Q}^{-1}), \quad (2.8)$$

which leaves the prior distribution $\mathcal{N}(\mathbf{0}, \mathbf{Q}^{-1})$ of the weights invariant. In order to sample $\boldsymbol{\gamma} \sim \mathcal{N}(\mathbf{0}, \mathbf{Q}^{-1})$ with large n_h it is important to leverage sparsity of \mathbf{Q} [35].

2.4 Our Criterion: Matching Posterior Contraction Rates

The FE approach outlined above involves a user-chosen hyperparameter h that affects both the estimation performance and computational cost. Smaller h leads to better approximation of the Matérn-type GP u by u_h and possibly enhanced inference, but renders a larger n_h that increases the computational cost. Since u_h is supposed to approximate the Matérn-type GP u , a natural choice for h is so that the estimation performance of using u_h as the prior is “comparable” to that of u . In this section we shall formalize such intuition with the notion of posterior contraction rates.

To begin with, recall that the goal is to infer the conditional expectation $f_0(\mathbf{x}) = \mathbb{E}[Y | \mathbf{X} = \mathbf{x}]$ from data $\{(\mathbf{X}_i, Y_i)\}_{i=1}^N$. We shall adopt a frequentist Bayesian perspective by putting a sequence of priors Π_N over f_0 and assuming that the data are indeed generated from a fixed f_0 which we interpret as the ground truth. Following [18], we say that the sequence of posteriors with respect to Π_N contracts around f_0 with rate ε_N if, for any sufficiently large $M > 0$,

$$\mathbb{E}_{f_0} \Pi_N \left(f : d_N(f, f_0) \leq M \varepsilon_N \mid \{(\mathbf{X}_i, Y_i)\}_{i=1}^N \right) \xrightarrow{N \rightarrow \infty} 1. \quad (2.9)$$

Here the expectation is taken with respect to the data distribution of $\{(\mathbf{X}_i, Y_i)\}_{i=1}^N$ determined by f_0 and the marginal of the \mathbf{X}_i 's, and d_N is a suitable discrepancy measure. Roughly speaking, ε_N is

the rate at which one can shrink the radius of a ball centered around the truth while at the same time capturing almost all the posterior mass. The condition (2.9) implies that asymptotically the sequence of posteriors will be nearly supported on a ball of radius $O(\varepsilon_N)$ around f_0 . Therefore, ε_N can be loosely interpreted as the convergence rate of the posteriors towards the truth. An important consequence [18, Theorem 2.5] is that the point estimator defined as

$$\widehat{f}_N = \arg \max_g \left[\Pi_N \left(f : d_N(f, g) \leq M\varepsilon_N \mid \{(\mathbf{X}_i, Y_i)\}_{i=1}^N \right) \right],$$

converges (in probability) to f_0 with the same rate ε_N . Therefore the contraction rate serves as a natural criterion for quantifying the estimation performance of the posteriors.

Following Subsection 2.3, the sequence of priors is taken as $\Pi_N = \text{Law}(u_{h_N})$ (resp. $\text{Law}(\Phi(u_{h_N}))$) for fixed design regression (resp. binary classification). The selection criterion for h_N that we propose is to choose h_N so that the sequence of posteriors with respect to Π_N contracts at the same rate as if $\Pi_N \equiv \Pi := \text{Law}(u)$ (resp. $\text{Law}(\Phi(u))$), where u is the Matérn-type GP that u_{h_N} is approximating. It turns out that there is a simple condition on the approximation accuracy of u_{h_N} towards u that guarantees this matching of posterior contraction rates, which we make precise below.

We start by reviewing the key ingredients of the theory when a single prior is adopted, i.e., when $\Pi_N \equiv \Pi$ in the above. Consider now u as a GP taking values in $(L^\infty(\mathcal{D}), \|\cdot\|_\infty)$ (see e.g. Lemma 3.6 below for conditions under which this is valid) for fixed design regression and in $(L^2(\mathcal{D}), \|\cdot\|_2)$ for binary classification. By [50, Theorems 3.2 and 3.3], the contraction rate with respect to Π in the fixed design regression (resp. binary classification) setting can be characterized as the sequence ε_N that satisfies $\varphi_{f_0}(\varepsilon_N; u, \|\cdot\|_\infty) \leq N\varepsilon_N^2$ (resp. $\varphi_{\Phi^{-1}(f_0)}(\varepsilon_N; u, \|\cdot\|_2) \leq N\varepsilon_N^2$), where

$$\varphi_{\omega_0}(\varepsilon; u, \|\cdot\|_{\mathbb{B}}) := \inf_{g \in \mathbb{H} : \|g - \omega_0\|_{\mathbb{B}} < \varepsilon} \|g\|_{\mathbb{H}}^2 - \log \mathbb{P}(\|u\|_{\mathbb{B}} < \varepsilon), \quad (2.10)$$

and $(\mathbb{H}, \|\cdot\|_{\mathbb{H}})$ denotes the *reproducing kernel Hilbert space* (RKHS) of Π (see e.g. [51] for more details). Under such circumstances, the sequence of posteriors with respect to Π contracts around f_0 with rate ε_N in the sense of (2.9) with $d_N = \|\cdot\|_N$ the empirical norm defined as $\|f\|_N^2 = N^{-1} \sum_{i=1}^N |f(\mathbf{X}_i)|^2$ for fixed design regression and $d_N = \|\cdot\|_2$ for binary classification. In other words, the posterior contraction rate can be determined by analyzing the so-called *concentration function* (2.10) of the prior. Now when a sequence of priors Π_N is used instead, it is reasonable to expect that if Π_N approximates Π sufficiently well, the concentration functions of Π_N will be close to that of Π so that the same contraction rate can be achieved. Indeed this is implied by [50, Theorems 2.2, 3.2 and 3.3], which we record as a proposition.

Proposition 2.2. *1. Fixed design regression: Let $\Pi_N = \text{Law}(u_{h_N})$. Suppose ε_N is a sequence of real numbers satisfying $\varphi_{f_0}(\varepsilon_N; u, \|\cdot\|_\infty) \leq N\varepsilon_N^2$ and*

$$10\mathbb{E}\|u_{h_N} - u\|_\infty^2 \leq N^{-1}. \quad (2.11)$$

Then, for any sufficiently large $M > 0$,

$$\mathbb{E}_{f_0} \Pi_N \left(f : \|f - f_0\|_N \leq M\varepsilon_N \mid \{(\mathbf{X}_i, Y_i)\}_{i=1}^N \right) \xrightarrow{N \rightarrow \infty} 1.$$

2. *Binary classification:* Let $\Pi_N = \text{Law}(\Phi(u_{h_N}))$. Suppose ε_N is a sequence of real numbers satisfying $\varphi_{\Phi^{-1}(f_0)}(\varepsilon_N; u, \|\cdot\|_2) \leq N\varepsilon_N^2$ and

$$10\mathbb{E}\|u_{h_N} - u\|_2^2 \leq N^{-1}. \quad (2.12)$$

Then, for any sufficiently large $M > 0$,

$$\mathbb{E}_{f_0}\Pi_N\left(f : \|f - f_0\|_2 \leq M\varepsilon_N \mid \{(\mathbf{X}_i, Y_i)\}_{i=1}^N\right) \xrightarrow{N \rightarrow \infty} 1.$$

Proposition 2.2 shows that the posteriors constructed with prior Π_N and with prior Π contract at the same rate, provided that the prior approximation is sufficiently accurate. Therefore it suffices to choose h_N so that (2.11) or (2.12) is satisfied, giving a simple criterion for setting h_N . In particular, if the error $\mathbb{E}\|u_{h_N} - u\|_\infty^2$ or $\mathbb{E}\|u_{h_N} - u\|_2^2$ decreases sufficiently fast, then a slowly decaying h_N is enough and leads to $n_{h_N} \asymp h_N^{-D} \ll N$. We will show in Section 3 for a simple linear FE method in a concrete setting that this is indeed the case under certain smoothness assumptions, and demonstrate such behavior through simulation studies in Section 4. Several possible extensions will be discussed in Section 5, building on the key idea of using Proposition 2.2 to balance the numerical error in the prior approximation with the statistical errors in regression and classification tasks.

3 Main Results

In this section we obtain sufficient scalings of n_h with respect to N using spectral error analysis for FE eigenvalue problems and our criterion outlined in Subsection 2.4. We assume throughout that $\mathcal{D} = (0, L_1) \times \cdots \times (0, L_D)$ is a hyperrectangle and that the Laplacian in (2.2) is supplemented with Neumann boundary condition, so that we have the following explicit expressions for its eigenvalues and eigenfunctions

$$\Lambda_{\mathbf{i}} = \sum_{d=1}^D \frac{i_d \pi}{L_d}, \quad \Psi_{\mathbf{i}}(\mathbf{x}) = C_{\mathbf{i}} \prod_{d=1}^D \cos\left(\frac{i_d \pi x_d}{L_d}\right), \quad (3.1)$$

where $\mathbf{i} = (i_1, \dots, i_D) \in \mathbb{N}^D$ is a multi-index and $C_{\mathbf{i}}$'s are constants so that the $\Psi_{\mathbf{i}}$'s are $L^2(\mathcal{D})$ -normalized. The Matérn-type GP (2.2) can then be written as

$$u = \kappa^{s-D/2} \sum_{\mathbf{i} \in \mathbb{N}^D} (\kappa^2 + \Lambda_{\mathbf{i}})^{-s/2} \xi_{\mathbf{i}} \Psi_{\mathbf{i}}, \quad \xi_{\mathbf{i}} \stackrel{i.i.d.}{\sim} \mathcal{N}(0, 1). \quad (3.2)$$

The explicit expressions for the eigenpairs in (3.1) allow us to establish the following result [26, Theorem 2.1], which shows that the covariance function of (3.2) is nearly indistinguishable from the classical Matérn covariance function (2.1) away from the boundary.

Proposition 3.1. *Let $c(\mathbf{x}, \mathbf{x}')$ denote the covariance function of the Matérn-type GP (3.2) and let $c_{\text{Mat}}(\mathbf{x}, \mathbf{x}')$ be the Matérn covariance function (2.1) with*

$$\sigma^2 = \frac{\Gamma(s - \frac{D}{2})}{(4\pi)^{D/2} \Gamma(s)}. \quad (3.3)$$

Then

$$c(\mathbf{x}, \mathbf{x}') = \sum_{\mathbf{k} \in \mathbb{Z}^D} \sum_{\mathbf{T} \in \mathcal{T}} c_{\text{Mat}}(\mathbf{T}\mathbf{x}, \mathbf{x}' - 2\mathbf{k}\mathbf{L}), \quad \mathbf{x}, \mathbf{x}' \in (0, L_1) \times \cdots \times (0, L_D), \quad (3.4)$$

where \mathcal{T} is the collection of all $D \times D$ diagonal matrices whose diagonal entries are either 1 or -1 , $\mathbf{T}\mathbf{x}$ denotes matrix-vector multiplication and $\mathbf{k}\mathbf{L}$ denotes $(k_1 L_1, \dots, k_D L_D)$.

Note that if the correlation range $\rho = \sqrt{8\nu}/\kappa$ (where, recall, $\nu = s - D/2$) is much smaller than $\min_d L_d$, and in addition \mathbf{x}, \mathbf{x}' are at a distance larger than 2ρ from each side of the hyperrectangle, the only significant term that remains in (3.4) is $c_{\text{Mat}}(\mathbf{x}, \mathbf{x}')$. Therefore, (3.2) gives a good approximation of the classical Matérn model away from the boundary. In practice one can choose a larger hyperrectangle than the domain of interest to reduce the boundary effect [28], see also [26]. Our focus on hyperrectangles also facilitates the concrete FE construction and error analysis in the next subsection.

3.1 FEM Construction and Spectral Error Bounds

We shall construct the FE space on $[0, L_1] \times \cdots \times [0, L_D]$ as the tensor product of FE spaces on each interval $[0, L_d]$. To begin with, let P be a uniform partition of $[0, L_d]$ into $K + 1$ points with width $h = L/K$ and let V_h be the space of continuous piecewise linear functions with respect to P . To simplify the notation we drop the dependence on d below. Precisely, a basis of V_h consists of

$$e_{h,k} = \begin{cases} h^{-1}x - k + 1 & x \in [(k-1)h, kh] \\ -h^{-1}x + k + 1 & x \in [kh, (k+1)h], \quad k = 1, \dots, K-1, \\ 0 & \text{otherwise} \end{cases}$$

with $e_{h,0} = (-h^{-1}x + 1)\mathbf{1}_{[0,h]}$ and $e_{K,h} = (h^{-1}x - K + 1)\mathbf{1}_{[(K-1)h, Kh]}$. Let \mathcal{J}_h be the Galerkin discretization of $\kappa^2 - \frac{d^2}{dx^2}$ over V_h . The eigenvalues $\{\lambda_{h,i}\}_{i=0}^K$ and eigenfunctions $\{\psi_{h,i}\}_{i=0}^K$ of \mathcal{J}_h can be found by solving the generalized eigenvalue problem

$$\mathbf{G}\mathbf{z} = \lambda\mathbf{M}\mathbf{z},$$

where \mathbf{z} represents the coordinates of $\psi_{h,i}$ in terms of the $e_{h,k}$'s and $\mathbf{G}, \mathbf{M} \in \mathbb{R}^{(K+1) \times (K+1)}$ are matrices with entries

$$\mathbf{G}_{ij} = \frac{1}{h} \cdot \begin{cases} 2 & i = j \notin \{1, K+1\} \\ 1 & i = j \in \{1, K+1\} \\ -1 & |i - j| = 1 \\ 0 & \text{otherwise} \end{cases}, \quad \mathbf{M}_{ij} = h \cdot \begin{cases} 2/3 & i = j \notin \{1, K+1\} \\ 1/3 & i = j \in \{1, K+1\} \\ 1/6 & |i - j| = 1 \\ 0 & \text{otherwise} \end{cases}.$$

One can check that

$$\lambda_{h,i} = \frac{6}{h^2} \frac{1 - \cos(i\pi h/L)}{2 + \cos(i\pi h/L)}, \quad \psi_{h,i} = c_i \sum_{k=0}^K \cos\left(\frac{ki\pi h}{L}\right) e_{h,k}, \quad i, k \in [K], \quad (3.5)$$

where c_i 's are normalizing constants so that $\psi_{h,i}$ has $L^2(\mathcal{D})$ norm one, and $[K] = \{0, \dots, K\}$. We then have the following error estimates:

Lemma 3.2. Let $\{(\lambda_i, \psi_i)\}_{i=1}^\infty$ be the eigenvalues and $L^2(\mathcal{D})$ -orthonormal eigenfunctions of $\kappa^2 - \frac{d^2}{dx^2}$ over $(0, L)$ with Neumann boundary condition. There is a constant C so that, for $i \in [K]$,

$$|\lambda_{h,i} - \lambda_i| \leq C\lambda_i^2 h^2, \quad \|\psi_{h,i} - \psi_i\|_\infty \leq C\lambda_i h^2.$$

Furthermore the $\psi_{h,i}$'s are also $L^2(\mathcal{D})$ -orthonormal.

Remark 3.3. Eigenvalue estimates and eigenfunction estimates in L^2 norm can be found for instance in [47, Theorems 6.1 and 6.2], where more general elliptic operators and domains are considered. However, for our subsequent developments we need eigenfunction estimates in L^∞ norm, and for this reason we include an elementary proof of Lemma 3.2 in Section 6. \square

For Galerkin discretization of $\kappa^2 - \Delta$ on $[0, L_1] \times \cdots \times [0, L_D]$, let \mathcal{P} be the uniform grid constructed by uniformly partitioning each interval with $K_d + 1$ nodes so that $h_d = L_d/K_d$ in each dimension. Define for $\mathbf{h} = (h_1, \dots, h_D)$ the FE space

$$\mathcal{V}_{\mathbf{h}} = V_{h_1} \otimes \cdots \otimes V_{h_D} := \left\{ v(\mathbf{x}) = \prod_{d=1}^D v_{h_d}(x_d) : v_{h_d} \in V_{h_d} \right\},$$

where V_{h_d} is the FE space on $[0, L_d]$ constructed above. It can be shown that the eigenvalues $\Lambda_{\mathbf{h}, \mathbf{i}}$ and eigenfunctions $\Psi_{\mathbf{h}, \mathbf{i}}$ of $\mathcal{L}_{\mathbf{h}}$ (the Galerkin discretization of $\kappa^2 - \Delta$) are

$$\Lambda_{\mathbf{h}, \mathbf{i}} = \sum_{d=1}^D \lambda_{h_d, i_d}, \quad \Psi_{\mathbf{h}, \mathbf{i}}(\mathbf{x}) = \prod_{d=1}^D \psi_{h_d, i_d}(x_d), \quad \mathbf{i} \in [K_1] \times \cdots \times [K_D],$$

where the λ_{h_d, i_d} 's and ψ_{h_d, i_d} 's are as in (3.5). Indeed for $v_{\mathbf{h}}(\mathbf{x}) = \prod_{d=1}^D v_{h_d}(x_d) \in \mathcal{V}_{\mathbf{h}}$ we have that

$$\begin{aligned} \langle \nabla \Psi_{\mathbf{h}, \mathbf{i}}, \nabla v_{\mathbf{h}} \rangle &= \int_{\mathcal{D}} \sum_{d=1}^D \left(\psi'_{h_d, i_d} v'_{h_d} \prod_{\ell \neq d} \psi_{h_\ell, i_\ell} v_{h_\ell} \right) d\mathbf{x} \\ &= \sum_{d=1}^D \langle \psi'_{h_d, i_d}, v'_{h_d} \rangle \prod_{\ell \neq d} \langle \psi_{h_\ell, i_\ell}, v_{h_\ell} \rangle = \sum_{d=1}^D \lambda_{h_d, i_d} \prod_{\ell=1}^D \langle \psi_{h_\ell, i_\ell}, v_{h_\ell} \rangle = \sum_{d=1}^D \lambda_{h_d, i_d} \langle \Psi_{\mathbf{h}, \mathbf{i}}, v_{\mathbf{h}} \rangle, \end{aligned}$$

where the primes denote weak derivatives. Moreover the $\Psi_{\mathbf{h}, \mathbf{i}}$'s are orthonormal since the $\psi_{h,i}$'s are and hence they form a complete set of eigenbasis for $\mathcal{L}_{\mathbf{h}}$. The following error estimates are immediate, where we recall that the true eigenpairs are given in (3.1):

Lemma 3.4. For $\mathbf{i} \in [K_1] \times \cdots \times [K_D]$ we have

$$|\Lambda_{\mathbf{h}, \mathbf{i}} - \Lambda_{\mathbf{i}}| \leq C\Lambda_{\mathbf{i}}^2 h^2, \quad \|\Psi_{\mathbf{h}, \mathbf{i}} - \Psi_{\mathbf{i}}\|_\infty \leq C\Lambda_{\mathbf{i}} h^2,$$

where $h = \max_d h_d$ and C is a constant depending only on D and the L_d 's.

Remark 3.5. Since \mathcal{D} is a bounded domain, we obtain also the $L^2(\mathcal{D})$ bound $\|\Psi_{\mathbf{h}, \mathbf{i}} - \Psi_{\mathbf{i}}\|_2 \leq C\Lambda_{\mathbf{i}} h^2$. \square

Since the approximation error in Lemma 3.4 depends on $h = \max_d h_d$, we shall from now on assume that the h_d 's are chosen so that they are of the same order, i.e., $\max_{j \neq k} \frac{h_j}{h_k} = O(1)$ as $h \rightarrow 0$, and treat only h as the mesh size. As a consequence the total number of grid points satisfies the following scaling

$$n_{\mathbf{h}} = \prod_{d=1}^D (L_d/h_d + 1) \asymp h^{-D}. \quad (3.6)$$

3.2 Balancing Numerical and Statistical Errors

Now we use the spectral error bounds in Lemma 3.4 to obtain $L^2(\mathcal{D})$ and $L^\infty(\mathcal{D})$ error bounds for FE representations of Matérn-type GP priors (Lemma 3.6). These prior bounds, combined with Proposition 2.2, will yield our main result (Theorem 3.8). Let

$$u_{\mathbf{h}} = \kappa^{s-D/2} \sum_{\mathbf{i} \in [K_1] \times \dots \times [K_D]} (\kappa^2 + \Lambda_{\mathbf{h},\mathbf{i}})^{-s/2} \xi_{\mathbf{i}} \Psi_{\mathbf{h},\mathbf{i}}, \quad \xi_{\mathbf{i}} \stackrel{i.i.d.}{\sim} \mathcal{N}(0, 1),$$

be the FE representation of the Matérn-type GP u in (3.2). Recall that we are interested in estimating the function $f_0(\mathbf{x}) = \mathbb{E}[Y|\mathbf{X} = \mathbf{x}]$ based on i.i.d. samples $\{(\mathbf{X}_i, Y_i)\}_{i=1}^N$ with prior $\Pi_N = \text{Law}(u_{\mathbf{h}_N})$ for the fixed design regression setting and $\Pi_N = \text{Law}(\Phi(u_{\mathbf{h}_N}))$ for the binary classification setting, where $\mathbf{h}_N = (h_{N,1}, \dots, h_{N,D})$ is to be determined. Based on the discussion in Subsection 2.4, it suffices to quantify the approximation error of u defined in (3.2) by $u_{\mathbf{h}_N}$.

Lemma 3.6. *Recall that $h = \max_d h_d$. Suppose $s > D/2$. It holds that*

$$\mathbb{E}\|u_{\mathbf{h}} - u\|_2^2 \leq C\kappa^{2s-D} h^{(2s-D)\wedge 4},$$

where C is a constant independent of κ and h . Furthermore the Matérn-type GP u defined in (3.2) belongs almost surely to $\mathcal{C}^\beta(\mathcal{D})$ for $0 < \beta < 1 \wedge (s - D/2)$. Moreover, for $s > D$ it holds that

$$\mathbb{E}\|u_{\mathbf{h}} - u\|_\infty^2 \leq C\kappa^{2s-D} h^{(2s-2D)\wedge 4},$$

where C is a constant independent of κ and h .

Remark 3.7. The L^2 error bound has been shown to hold in greater generality, see e.g. [3, Theorem 2.10] and [7, Theorem 2]. A sharper L^∞ error bound was shown in [7, Theorem 3] when $D = 1$, while our result holds for general dimension D .

As a corollary of Proposition 2.2 we have the following main result, presented in terms of the scaling of $h_N = \max_d h_{N,d}$. Notice that the concentration function defined in (2.10) depends implicitly on s through u .

Theorem 3.8. *1. Fixed design regression: Consider the Matérn-type GP u defined by (2.3) with $s > D$. Suppose ε_N satisfies $\varphi_{f_0}(\varepsilon_N; u, \|\cdot\|_\infty) \leq N\varepsilon_N^2$. Set*

$$h_N \asymp N^{-\frac{1}{(2s-2D)\wedge 4}} \tag{3.7}$$

with a large enough proportion constant. Then, for any sufficiently large $M > 0$,

$$\mathbb{E}_{f_0} \Pi_N \left(f : \|f - f_0\|_N \leq M\varepsilon_N \mid \{(\mathbf{X}_i, Y_i)\}_{i=1}^N \right) \xrightarrow{N \rightarrow \infty} 1,$$

where we recall $\|f\|_N^2 = N^{-1} \sum_{i=1}^N |f(\mathbf{X}_i)|^2$.

2. Binary classification: Consider the Matérn-type GP u defined by (2.3) with $s > D/2$. Suppose ε_N satisfies $\varphi_{\Phi^{-1}(f_0)}(\varepsilon_N; u, \|\cdot\|_2) \leq N\varepsilon_N^2$. Set

$$h_N \asymp N^{-\frac{1}{(2s-D)\wedge 4}} \tag{3.8}$$

with a large enough proportion constant. Then, for any sufficiently large $M > 0$,

$$\mathbb{E}_{f_0} \Pi_N \left(f : \|f - f_0\|_2 \leq M\varepsilon_N \mid \{(\mathbf{X}_i, Y_i)\}_{i=1}^N \right) \xrightarrow{N \rightarrow \infty} 1.$$

Remark 3.9. Theorem 3.8 provides a scaling of h_N so that the sequence of posteriors with respect to the FE prior Π_N achieves the same contraction rate as if the Matérn-type prior Π was used. We remark that a refined analysis of the rate at which the posterior probabilities go to 1 could be used to obtain similar conclusions for the posterior means under suitable assumptions, i.e.

$$\begin{aligned}\mathbb{E}_{f_0} d_N(\hat{f}, f_0)^2 &\lesssim \varepsilon_N^2, & \hat{f} &= \int f d\Pi(f|\{(\mathbf{X}_i, Y_i)\}_{i=1}^N), \\ \mathbb{E}_{f_0} d_N(\hat{f}_N, f_0)^2 &\lesssim \varepsilon_N^2, & \hat{f}_N &= \int f d\Pi_N(f|\{(\mathbf{X}_i, Y_i)\}_{i=1}^N).\end{aligned}$$

In other words, the sequence of posterior means with respect to Π_N converges to f_0 at the same rate as those with respect to Π , thereby giving a more interpretable conclusion. For fixed design regression, this follows from [52, Theorem 1] and Jensen's inequality with $d_N = \|\cdot\|_N$. For binary classification, using again Jensen's inequality and the fact that $|f| \leq 1$ we have

$$\begin{aligned}\|\hat{f} - f_0\|_2^2 &\leq \int \|f - f_0\|_2^2 d\Pi(f|\{(\mathbf{X}_i, Y_i)\}_{i=1}^N) \\ &\leq M^2 \varepsilon_N^2 + 4|\mathcal{D}|\Pi(f : \|f - f_0\|_2 \geq M\varepsilon_N|\{(\mathbf{X}_i, Y_i)\}_{i=1}^N),\end{aligned}$$

where $|\mathcal{D}|$ is the Lebesgue measure of \mathcal{D} . Therefore a rate faster than ε_N^2 on the decay of the posterior probability suffices, which is satisfied under mild assumptions [18, Theorems 2.2 and 2.3]. \square

Remark 3.10. For the regression setting, (3.7) together with (3.6) gives the scaling for the total number of grid points needed,

$$n_{\mathbf{h}_N} \asymp N^{\frac{D}{(2s-2D)\wedge 4}}.$$

In particular when $s > 3D/2$, $D = 1, 2, 3$, the exponent for N is less than one and we have $n_{\mathbf{h}_N} \ll N$ asymptotically. For classification, $s > D$ suffices. However, we remark that the proportion constant depends implicitly on κ and the L_d 's as can be seen from (3.6) and Lemma 3.6. In particular, if both κ and the L_d 's are large, which reflects the case of a rapidly changing field over a large spatial domain, then N may need to be large enough in order for $n_{\mathbf{h}_N}$ to be smaller than N . We shall demonstrate through simulation studies in Section 4 that for moderate κ and L_d 's one can achieve $n_{\mathbf{h}} < N$ when $N = O(10^2)$ for a one-dimensional example and $N = O(10^3)$ for a two-dimensional one, thereby suggesting that Theorem 3.8 has some practical implication. \square

The scaling of h_N in Theorem 3.8 ensures that the numerical errors in the FE representations of a true Matérn-type GPs u do not impact the corresponding contraction rates. In the remainder of this section we give an example where the rates ε_N with respect to the true Matérn-type GP u can be explicitly computed under a smoothness assumption on the truth f_0 . For this purpose we introduce a notion of regularity of f_0 based on the orthonormal basis $\{\Psi_{\mathbf{i}}\}_{\mathbf{i} \in \mathbb{N}^D}$. Let S be an even function in the Schwartz space $\mathcal{S}(\mathbb{R})$ satisfying

$$0 \leq S \leq 1, \quad S \equiv 1 \text{ on } \left[-\frac{1}{2}, \frac{1}{2}\right], \quad \text{supp}(S) \subset [-1, 1].$$

Define the space

$$B_{\infty,\infty}^{\beta} = \left\{ f = \sum_{\mathbf{i} \in \mathbb{N}^D} f_{\mathbf{i}} \Psi_{\mathbf{i}} : \|f\|_{B_{\infty,\infty}^{\beta}} = \sup_{j \in \mathbb{N}} 2^{\beta j} \|S_j(\sqrt{\Delta})f(\cdot) - f(\cdot)\|_{\infty} < \infty \right\},$$

where $S_j(\cdot) = S(2^{-j}\cdot)$ and

$$S_j(\sqrt{\Delta})f = \sum_{\mathbf{i} \in \mathbb{N}^D} S_j(\sqrt{\Lambda_{\mathbf{i}}})f_{\mathbf{i}} \Psi_{\mathbf{i}}.$$

Proposition 3.11. *Suppose $f_0 \in B_{\infty,\infty}^{\beta}$ and set $s = \beta + \frac{D}{2}$ in the definition of u . Then for ε_N a large enough multiple of $N^{-\beta/(2\beta+D)}$, we have $\varphi_{f_0}(\varepsilon_N; u, \|\cdot\|_2) \leq N\varepsilon_N^2$ and $\varphi_{f_0}(\varepsilon_N; u, \|\cdot\|_{\infty}) \leq N\varepsilon_N^2$.*

The space $B_{\infty,\infty}^{\beta}$ can be seen as a Besov-type space tailored to our specific setting, where the prior support associated with the Matérn-type GP u consists of functions defined as series expansions in terms of the $\Psi_{\mathbf{i}}$'s. Similar function spaces have been considered in [5]. As the usual Besov spaces, functions in $B_{\infty,\infty}^{\beta}$ should be understood to have regularity of order β , in which case the contraction rate $N^{-\beta/(2\beta+D)}$ matches the usual minimax optimal rate for estimating β -regular functions.

4 Simulation Study

The aim of this section is to complement the understanding given by Theorem 3.8 through numerical simulations in the regression setting. We consider one and two-dimensional examples in Subsections 4.1 and 4.2, respectively.

The general set up is as follows. Let $\{\mathbf{X}_i\}_{i=1}^N$ be fixed design points in the domain \mathcal{D} and $\{Y_i\}_{i=1}^N$ be noisy observations generated from

$$Y_i = f_0(\mathbf{X}_i) + \eta_i, \quad \eta_i \stackrel{i.i.d.}{\sim} \mathcal{N}(0, \tau^2),$$

where f_0 is the ground truth and τ is known. We compare two approaches for inferring f_0 , namely the covariance function (CF) approach and the finite element (FE) approach with mass lumping. They can be summarized as follows:

$$\mathbf{y} \sim \mathcal{N}(\mathbf{f}_N, \tau^2 I_N), \quad \mathbf{f}_N \sim \mathcal{N}(\mathbf{0}, \Sigma) \implies \hat{\mathbf{f}}_{\text{CF}} = \Sigma(\Sigma + \tau^2 \mathbf{I}_N)^{-1} \mathbf{y},$$

where $\Sigma = \{c_{\text{Mat}}(\mathbf{X}_i, \mathbf{X}_j)\}$; and

$$\mathbf{y} \sim \mathcal{N}(\mathbf{S}\mathbf{w}, \tau^2 I_N), \quad \mathbf{w} \sim \mathcal{N}(\mathbf{0}, \mathbf{Q}^{-1}) \implies \hat{\mathbf{f}}_{\text{FE}} = \mathbf{S}(\mathbf{S}^{\top} \mathbf{S} + \tau^2 \mathbf{Q})^{-1} \mathbf{S}^{\top} \mathbf{y},$$

where $\mathbf{S}_{ij} = e_j(X_i)$ is as in Subsection 2.3 and $\mathbf{Q} = (\kappa^2 \mathbf{M} + \mathbf{G}) [\widetilde{\mathbf{M}}^{-1} (\kappa^2 \mathbf{M} + \mathbf{G})]^{s-1}$ as in Proposition 2.1 but with the lumped mass matrix $\widetilde{\mathbf{M}}$ instead. As noted in Remark 3.9, we shall compare the error $\|\hat{\mathbf{f}}_{\text{CF}} - \mathbf{f}_0\|_N$ and $\|\hat{\mathbf{f}}_{\text{FE}} - \mathbf{f}_0\|_N$ when an increasing number of grid points (n_h) is used in the FE approach, where $\mathbf{f}_0 = (f_0(\mathbf{X}_1), \dots, f_0(\mathbf{X}_N))^{\top}$ and $\|\cdot\|_N$ is the vector 2-norm normalized by $1/\sqrt{N}$. Note that the CF and FE approaches studied here are not exactly those analyzed in Theorem 3.8, i.e., the error of going from the CF approach to the Matérn-type prior (expected to be small by Proposition 3.1) and that of the lumped mass procedure were not accounted for. However, we remark that both errors do not lead to a significant difference in the numerical results and we will only focus on the CF and FE approaches, which are used in practice.

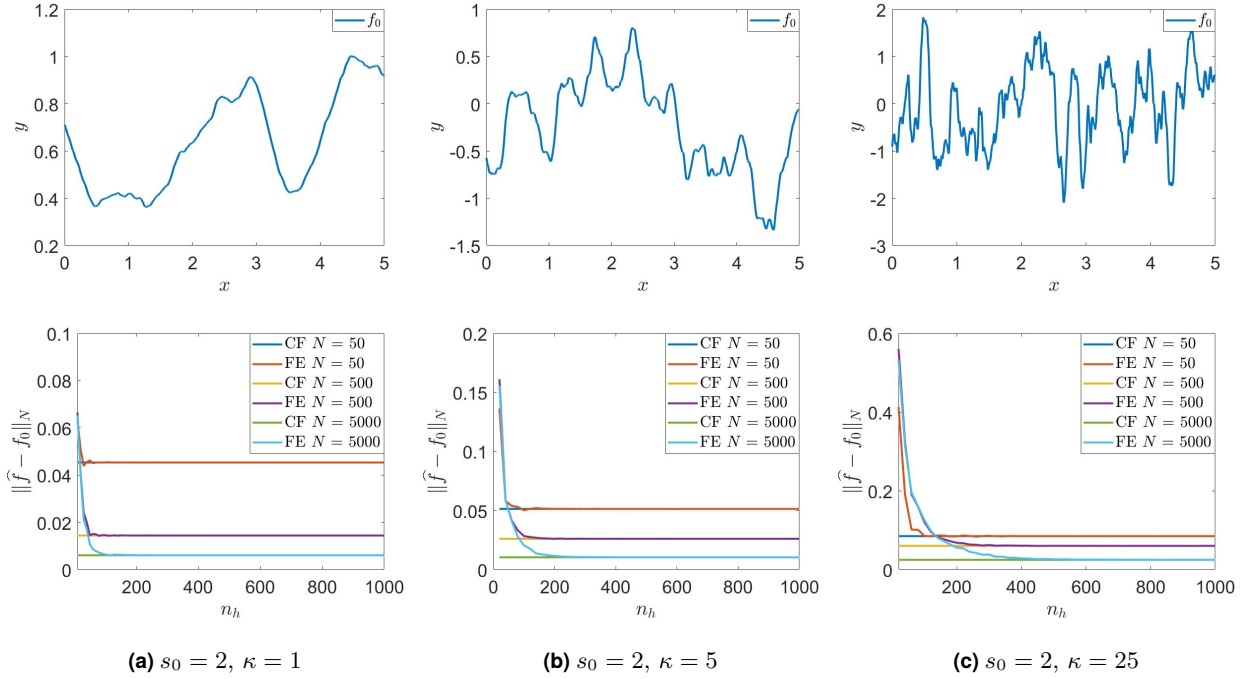


Figure 1 The three columns represent simulations for $\kappa_0 = 1, 5$ and 25 respectively with $s_0 = 2$ in all cases. The upper row shows plots of f_0 . The lower row compares the estimation error $\|\hat{\mathbf{f}} - \mathbf{f}_0\|_N$ between the covariance function (CF) approach and the finite element (FE) approach as n_h increases, for three levels of data $N = 50, 500$ and 5000 .

4.1 The One-dimensional Case

To start with, let $\{\mathbf{X}_i\}_{i=1}^N$ be fixed design points generated from the uniform distribution over $[0, L]$. We shall consider f_0 's generated from the following series expansion (with a sufficiently high truncation)

$$f_0(x) \sim \frac{\kappa_0^{-1/2} \xi_0}{\sqrt{L}} + \frac{\sqrt{2} \kappa_0^{s_0-1/2}}{\sqrt{L}} \sum_{i=1}^{\infty} \left[\kappa_0^2 + \left(\frac{i\pi}{L} \right)^2 \right]^{-s_0/2} \left[\xi_i \cos\left(\frac{i\pi x}{L} \right) + \zeta_i \sin\left(\frac{i\pi x}{L} \right) \right], \quad (4.1)$$

where $\xi_i, \zeta_i \stackrel{i.i.d.}{\sim} \mathcal{N}(0, 1)$. Notice that (4.1) is defined in the same spirit as (2.3) except that the full trigonometric basis is used, so that the random field (4.1) does not have a prescribed boundary condition. Our motivation to not consider here a Neumann boundary condition is to illustrate that similar conclusions as those suggested by our theory can be expected in more general settings. Notice again that there are two parameters s_0 and κ_0 , which control the smoothness and correlation lengthscale respectively. We will vary both s_0 and κ_0 in the following simulations.

For both the CF and FE approaches, we use the same parameters s_0 and κ_0 that are used to generate f_0 . In other words, we consider the Matérn covariance (2.1) with parameters $\nu = s_0 - 1/2$, $\kappa = \kappa_0$ and σ^2 given in (3.3), and FE approximation (2.5) with $s = s_0$ and $\kappa = \kappa_0$. For the FE approach, we construct the approximation over the larger interval $[-\rho, L + \rho]$ where $\rho = \sqrt{8\nu}/\kappa$ to reduce the boundary effects suggested in Proposition 3.1. Three levels of data $N = 50, 500$ and

5000 are considered and, for each N , we study the performance for the FE approach as the number n_h of grid points increases. Finally we let $L = 5$ and $\tau = 0.1 \cdot \|\mathbf{f}_0\|_2 / \sqrt{N}$, which amounts to about 10% error.

Figure 1 shows the results when we fix the smoothness $s_0 = 2$ and vary $\kappa_0 = 1, 5$ and 25. We see that the estimation error for the FE approach decreases to that of the CF approach after certain threshold n_h^* . In other words, discretization at the level of n_h^* for the FE approach is sufficient to yield the same estimation performance as the CF approach. The value of n_h^* is seen to be smaller than the sample size when $N = 500$ and is of an order of magnitude smaller when $N = 5000$, in the same spirit as the scaling suggested in Theorem 3.8. The fact that n_h^* is larger than the sample size when $N = 50$ can be explained by the large proportion constant in Remark 3.10. Furthermore such proportion constant increases with κ , as suggested by the larger n_h^* for a larger κ .

To further understand the effect of the smoothness s_0 , we perform two more simulations for (a) $s_0 = 1, \kappa_0 = 1$ and (b) $s_0 = 3, \kappa_0 = 25$. For (a) we see in Figure 2a that the n_h^* 's in this case are much larger than the $s_0 = 2$ cases. This is due to the roughness of the truth and the prior used and hence a large number of grid points are needed for accurate approximation even if κ is small. On the other hand when $s_0 = 3$, Figure 2b shows qualitatively similar results as in Figure 1 in the sense that n_h^* is asymptotically much smaller than N . Moreover the n_h^* 's are seen to be smaller than those when $s_0 = 2, \kappa_0 = 25$, as the underlying field is smoother and the required scaling suggested by Theorem 3.8 is smaller.

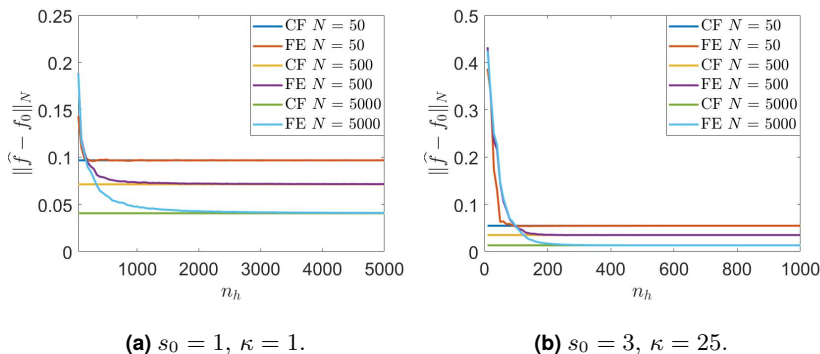


Figure 2 Comparison of estimation error $\|\hat{\mathbf{f}} - \mathbf{f}_0\|_N$ between the covariance function (CF) approach and the finite element (FE) approach on three data levels $N = 50, 500, 5000$ for (a) $s_0 = 1, \kappa = 1$ and (b) $s_0 = 3, \kappa = 25$.

4.2 The Two-dimensional Case

Now we move on to the more practically relevant two-dimensional case following a similar set up as above. Let $\{\mathbf{X}_i\}_{i=1}^N$ be fixed design points generated from the uniform distribution over the square $[0, L]^2$ and f_0 be generated similarly as (2.3) with ψ_i 's the full trigonometric basis (i.e. elements of the form $\sin(10\pi x_1/L) \sin(5\pi x_2/L)$, $\cos(3\pi x_1/L) \sin(9\pi x_2/L)$, etc.) so that there is no prescribed boundary condition for f_0 . We shall again compare the CF and FE approaches when f_0 is generated with different values of s_0 and κ_0 .

The exact procedure for the CF and FE approaches will be completely analogous to the 1D case. In particular, the same parameters s_0 and κ_0 that generate f_0 are used and furthermore the FE

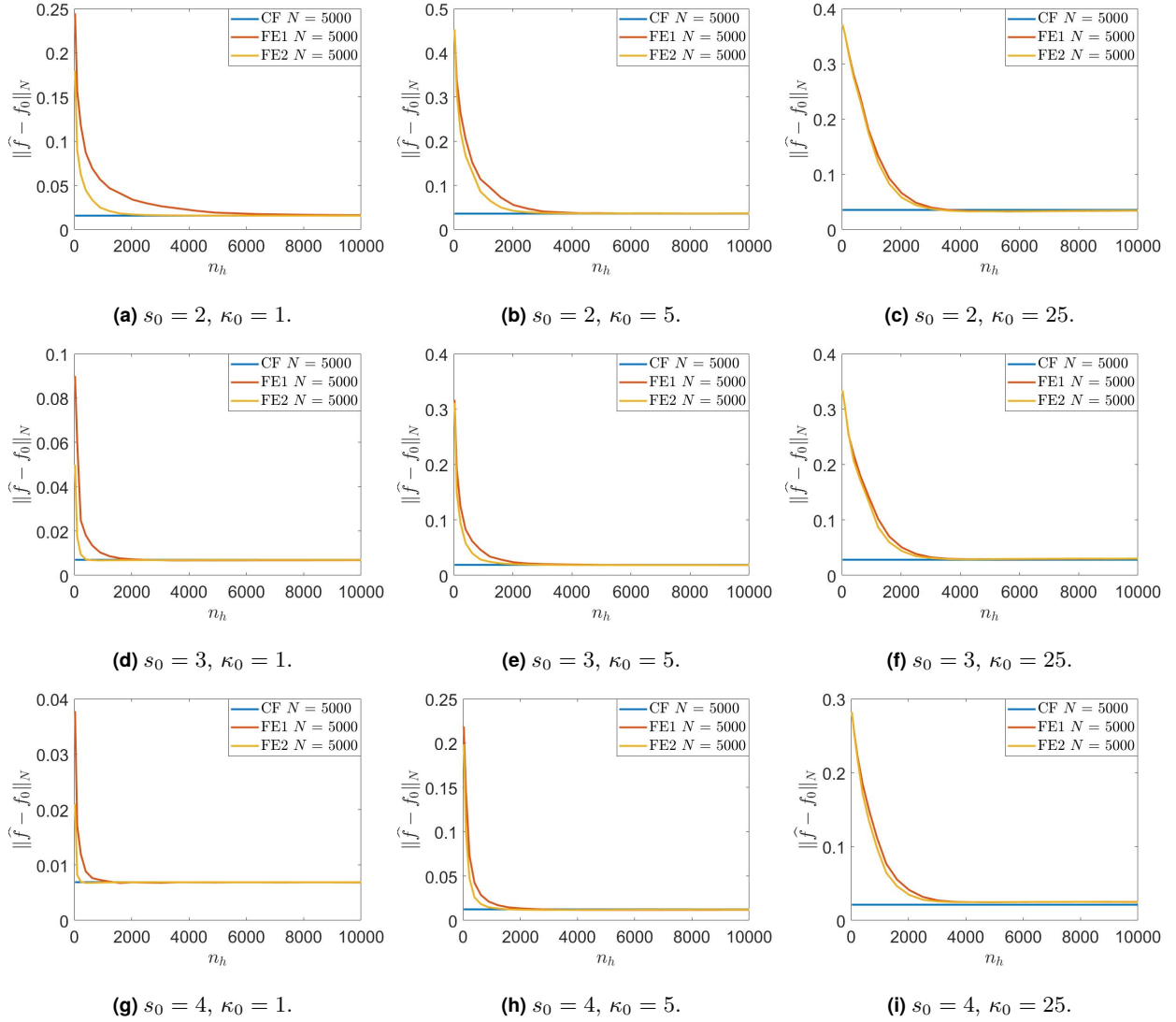


Figure 3 Comparison of the estimation error $\|\hat{\mathbf{f}} - \mathbf{f}_0\|_N$ as n_h increases between the covariance function (CF) approach and two finite element approaches where FE1 is computed over $[-\rho, L + \rho]^2$ and FE2 is computed over $[-0.1\rho, L + 0.1\rho]^2$. Simulation results for different combinations of s_0 and κ_0 are shown.

approach is carried out over the larger domain $[-\rho, L + \rho]^2$ with $\rho = \sqrt{8\nu}/\kappa$ to reduce boundary effects. However we remark that in the 2D case extending the domain has a larger impact on the performance of the FE approach than the 1D case. The reason is that to achieve the same mesh size within the domain $[0, L]^2$, the FE approach over $[-\rho, L + \rho]^2$ will require many more grid points than over $[0, L]^2$. In particular if a uniform partition of mesh size h as in Subsection 3.1 is adopted, then the overall increment of number of grid points is

$$\left(\frac{L + 2\rho}{h}\right)^2 - \left(\frac{L}{h}\right)^2 = \left(\frac{2\rho}{h}\right)\left(\frac{2L}{h}\right) + \left(\frac{\rho}{h}\right)^2. \quad (4.2)$$

The factor $2L/h$ makes (4.2) much larger than the increment $2\rho/h$ in each dimension and leads to a much larger saturation threshold n_h^* (that we have introduced in Subsection 4.1). For this reason we consider an alternate FE approach carried out over the smaller domain $[-0.1\rho, L + 0.1\rho]^2$ and compare its performance with the other FE approach over $[-\rho, L + \rho]^2$. For the simulations that we are going to present, we fix $N = 5000$, $L = 5$, $\tau = 0.1 \cdot \|\mathbf{f}_0\|_2/\sqrt{N}$ and vary $s_0 \in \{2, 3, 4\}$, $\kappa_0 \in \{1, 5, 25\}$, where we recall $\mathbf{f}_0 = (f_0(\mathbf{X}_1), \dots, f_0(\mathbf{X}_N))^\top$. Similar parameter settings were considered in [2].

Figure 3 shows qualitatively similar results as those in Subsection 4.1, where the estimation error of both FE approaches decreases to that of the CF approach after certain threshold n_h^* . Although Theorem 3.8 suggests a smaller asymptotic scaling for n_h^* only when $s > 3$, the simulation results suggest that this is true for $s = 3$ and even for $s = 2$ when the FE approach is computed over $[-0.1\rho, L + 0.1\rho]^2$. Furthermore, no estimation accuracy is lost when this smaller domain is used and a smaller n_h^* suffices so that it is more favorable, especially when κ is small or equivalently when ρ is large. Finally we remark that $s_0 = 2, \kappa_0 = 25$ corresponds to a very rapidly changing field and even in this case we have $n_h^* < N$ when $N = 5000$, which is also a realistic amount of data relative to the domain size. Following the same intuition as provided in Figure 1, it is reasonable to expect that one can take n_h an order of magnitude smaller than N when e.g. $N = 50000$. Therefore we believe the results in Theorem 3.8 have practical implications for a wide range of moderate nonasymptotic regimes and can provide some meaningful insights for real world applications.

5 Discussion and Open Directions

In this paper we have employed a Bayesian nonparametrics framework to provide new understanding on the choice of the dimension n_h in FE approaches to GP regression and classification. Our theory and simulation studies demonstrate that under mild smoothness assumptions one can take $n_h \ll N$ for a wide range of practical scenarios without hindering the estimation accuracy, leading to a second layer of computational gain on top of the well-celebrated sparsity provided by the FE approach.

One of the key elements in our analysis is the framework [50] which allows to translate prior approximation guarantees to the posteriors. In the context of GP regression and classification, this boils down to controlling, respectively, the error $\mathbb{E}\|u_{h_N} - u\|_\infty^2$ and $\mathbb{E}\|u_{h_N} - u\|_2^2$ as in Proposition 2.2. In Sections 3 and 4 we have used this framework to analyze the Matérn covariance approach and linear FE approximations thereof on a hyperrectangle. We remark that the applicability of our framework goes beyond this simple setting with the following possible extensions.

General Elliptic Operators One can define a nonstationary Matérn-type GP similarly as in (2.2) by replacing the operator $\kappa^2 - \Delta$ with a more general elliptic operator $\kappa^2 - \nabla \cdot (\mathbf{H}\nabla)$ on a general domain, where κ and \mathbf{H} are smooth functions taking values in real numbers and matrices, respectively. The error analysis in [3, 7] on FE approximations of these random fields together with Proposition 2.2 would give a sufficient scaling of the mesh size h_N . We remark that in this case there would not be an easily computable covariance function approach to compare with, but one can still arrive at the conclusion that there is no need to discretize beyond the threshold implied by Proposition 2.2.

Higher Order FEM Higher order finite elements may be employed when the smoothness parameter s is large. In particular, results from [3, 7] show that the L^2 approximation rate in Lemma 3.6 can be improved to $h^{(2s-D)\wedge(2p+2)}$ when polynomials of order p are used. As a result, the scaling for h_N in Theorem 3.8 can be improved accordingly. The L^∞ approximation rate for $p > 1$ remains an

interesting open question.

Rational Approximation When the smoothness parameter s is not an integer, the favorable sparsity of the FE approximation is lost. For this reason, [1] proposed a rational approximation of the fractional operator which retains sparsity. The resulting approximate field is shown to satisfy a similar L^2 approximation error bound as in Lemma 3.6, with an additional term coming from the rational approximation which can be made as small as desired. Following a similar argument as in [1], our proof for the L^∞ bound can also be extended to the rational approximate field. These prior approximation rates can again be combined with Proposition 2.2 to yield a sufficient scaling of the mesh size.

Learning the Lengthscale A novel aspect of our error bounds for FE prior representations is that we keep track of the (inverse) lengthscale parameter κ . Our theory and numerical experiments help explain the need of finer discretization when the lengthscale is shorter. An interesting direction for further research is the design of algorithms for the simultaneous learning of (i) adaptive FE meshes for GP representations; and (ii) spatially-variable lengthscale parameters $\kappa(x)$ in nonstationary Matérn-type models.

Beyond Regression and Classification Lastly, we also envision that the framework we have introduced can be adopted in other problems such as density estimation [18] and nonlinear Bayesian inverse problems [48]. The results from [50] readily extend our framework to density estimation problems and it is an interesting direction to extend Proposition 2.2 to Bayesian inverse problem settings building, for instance, on [31, 19].

6 Proof of Main Results

Proof of Proposition 2.1. It suffices to find the coordinates of (2.5) in terms of the finite element basis $e_{h,i}$'s. Taking inner product of (2.5) with $e_{h,j}$, we get

$$\sum_{i=1}^{n_h} (\kappa^2 + \lambda_{h,i})^{-s/2} \xi_i \langle \psi_{h,i}, e_{h,j} \rangle = \sum_{i=1}^{n_h} w_i \langle e_{h,i}, e_{h,j} \rangle \quad j = 1, \dots, n_h,$$

and the system

$$\mathbf{R}(\kappa^2 \mathbf{I}_{n_h} + \mathbf{\Lambda})^{-s/2} \boldsymbol{\xi} = \mathbf{M} \mathbf{w}, \quad (6.1)$$

where $\mathbf{R}_{ij} = \langle e_{h,i}, \psi_{h,j} \rangle$ and $\mathbf{\Lambda}$ is the diagonal matrix with entries $\mathbf{\Lambda}_{ii} = \lambda_{h,i}$. It now remains to relate $\mathbf{\Lambda}$ with the matrices $\mathbf{R}, \mathbf{M}, \mathbf{G}$. Since the $\psi_{h,i}$'s form an orthonormal basis, we have $e_{h,i} = \sum_{j=1}^{n_h} \langle e_{h,i}, \psi_{h,j} \rangle \psi_{h,j} = \sum_{j=1}^{n_h} \mathbf{R}_{ij} \psi_{h,j}$, which implies that $\psi_{h,i} = \sum_{j=1}^{n_h} (\mathbf{R}^{-1})_{ij} e_{h,j}$. The fact that $\psi_{h,i}$'s are (variational) eigenvectors of $-\Delta_h$ with corresponding eigenvalues $\lambda_{h,i}$ gives $\mathbf{G} \mathbf{R}^{-\top} = \mathbf{M} \mathbf{R}^{-\top} \mathbf{\Lambda}$, which together with the fact that $\mathbf{R} \mathbf{R}^\top = \mathbf{M}$ further implies $\mathbf{\Lambda} = \mathbf{R}^{-1} \mathbf{G} \mathbf{R}^{-\top}$. The result then follows by plugging such representation for $\mathbf{\Lambda}$ into (6.1). \square

Proof of Lemma 3.2. First note that we have $\lambda_0 = 0$, $\psi_0 \equiv 1/L$ and

$$\lambda_i = \left(\frac{i\pi}{L} \right)^2, \quad \psi_i = \frac{2}{L} \cos\left(\frac{i\pi x}{L} \right), \quad i = 1, 2, \dots$$

We then have

$$\begin{aligned} |\lambda_{h,i} - \lambda_i| &\leq \frac{1}{2 + \cos(i\pi h/L)} \left| \frac{6}{h^2} \left(1 - \cos \frac{i\pi h}{L}\right) - \left(\frac{i\pi}{L}\right)^2 \left(2 + \cos \frac{i\pi h}{L}\right) \right| \\ &\leq \left| \frac{6}{h^2} \left(1 - \cos \frac{i\pi h}{L}\right) - \left(\frac{i\pi}{L}\right)^2 \left(2 + \cos \frac{i\pi h}{L}\right) \right|. \end{aligned}$$

Expanding the last expression based on the Taylor series of $\cos x$ we obtain

$$|\lambda_{h,i} - \lambda_i| \leq \left| \frac{3}{h^2} \left(\frac{i\pi h}{L}\right)^2 + \frac{1}{h^2} O\left(\frac{i\pi h}{L}\right)^4 - 3\left(\frac{i\pi}{L}\right)^2 + \left(\frac{i\pi}{L}\right)^2 O\left(\frac{i\pi h}{L}\right)^2 \right| \leq C\lambda_i^2 h^2.$$

For the approximation error of the eigenfunctions, we first compute the normalizing constants c_i 's. For $i = 0$ we notice that $\psi_{h,0}$ is constant and hence $c_0 = 1/L$. For general i 's, we denote $\psi_{h,i} = \sum_{k=0}^K z_{h,i,k} e_{h,k}$ and compute

$$\begin{aligned} \langle \psi_{h,i}, \psi_{h,j} \rangle &= \sum_{k=0}^K \sum_{\ell=0}^K z_{h,i,k} z_{h,j,\ell} \langle e_{h,k}, e_{h,\ell} \rangle \\ &= z_{h,i,0} \sum_{\ell=0}^K z_{h,j,\ell} \langle e_{h,0}, e_{h,\ell} \rangle + z_{h,i,K} \sum_{\ell=0}^K z_{h,j,\ell} \langle e_{h,K}, e_{h,\ell} \rangle + \sum_{k=1}^{K-1} z_{h,i,k} \sum_{\ell=0}^K z_{h,j,\ell} \langle e_{h,k}, e_{h,\ell} \rangle \\ &= z_{h,i,0} \left(\frac{z_{h,j,0}}{3} + \frac{z_{h,j,1}}{6} \right) h + z_{h,i,K} \left(\frac{z_{h,j,K}}{3} + \frac{z_{h,j,K-1}}{6} \right) h \\ &\quad + \sum_{k=1}^{K-1} z_{h,i,k} \left(\frac{z_{h,j,k-1}}{6} + \frac{2z_{h,j,k}}{3} + \frac{z_{h,j,k+1}}{6} \right) h \\ &= c_i c_j h \left(\frac{1}{6} \cos \frac{j\pi h}{L} + \frac{1}{3} \right) \left[1 + (-1)^{i+j} + 2 \sum_{k=1}^{K-1} \cos\left(\frac{ki\pi h}{L}\right) \cos\left(\frac{kj\pi h}{L}\right) \right], \end{aligned}$$

where we have used that $\cos(a-t) + \cos(a+t) = 2\cos(a)\cos(t)$. Using further the fact that $2\cos(a)\cos(b) = \cos(a+b) + \cos(a-b)$, we have

$$2 \sum_{k=1}^{K-1} \cos\left(\frac{ki\pi h}{L}\right) \cos\left(\frac{kj\pi h}{L}\right) = \sum_{k=1}^{K-1} \cos\left(\frac{k(i+j)\pi h}{L}\right) + \cos\left(\frac{k(i-j)\pi h}{L}\right).$$

Now letting $t = (i+j)\pi h/L$ and denoting ι as the imaginary unit, we have

$$\begin{aligned} \sum_{k=1}^{K-1} \cos(kt) &= \frac{1}{2} \sum_{k=1}^{K-1} e^{\iota kt} + e^{-\iota kt} = \frac{1}{2} \left[\frac{e^{\iota t}(1 - e^{\iota(K-1)t})}{1 - e^{\iota t}} + \frac{e^{-\iota t}(1 - e^{-\iota(K-1)t})}{1 - e^{-\iota t}} \right] \\ &= -\frac{1}{2} [1 + (-1)^{i+j}], \end{aligned}$$

where we have used that $Kt = (i+j)\pi$. Similarly, we have

$$\sum_{k=1}^{K-1} \cos\left(\frac{k(i-j)\pi h}{L}\right) = \begin{cases} -\frac{1}{2} [1 + (-1)^{i-j}] & i \neq j \\ K-1 & i = j \end{cases}.$$

Therefore we have

$$\langle \psi_{h,i}, \psi_{h,j} \rangle = c_i c_j L \left(\frac{1}{6} \cos \frac{j\pi h}{L} + \frac{1}{3} \right) \delta_{ij},$$

where δ_{ij} denotes the Kronecker delta. Therefore the $\psi_{h,i}$'s are orthonormal with

$$c_i = \left[L \left(\frac{1}{6} \cos \frac{i\pi h}{L} + \frac{1}{3} \right) \right]^{-1/2}.$$

Now to bound the eigenfunction approximation error, we have

$$\|\psi_{h,i} - \psi_i\|_\infty \leq \|\psi_{h,i} - \tilde{\psi}_{h,i}\|_\infty + \|\tilde{\psi}_{h,i} - \psi_i\|_\infty,$$

where $\tilde{\psi}_{h,i} = \frac{1}{c_i} \sqrt{\frac{2}{L}} \psi_{h,i}$. Since $\|\psi_{h,i}\|_\infty \leq 1$, we have

$$\|\psi_{h,i} - \tilde{\psi}_{h,i}\|_\infty \leq \left| 1 - \frac{1}{c_i} \sqrt{\frac{2}{L}} \right| \leq C \left| L \left(\frac{1}{6} \cos \frac{i\pi h}{L} + \frac{1}{3} \right) - \frac{L}{2} \right| \leq C \left(\frac{i\pi h}{L} \right)^2 = C \lambda_i h^2,$$

where C is constant depending only on L . To bound $\|\tilde{\psi}_{h,i} - \psi_i\|_\infty$, notice that after the rescaling, $\tilde{\psi}_{h,i}$ is a linear interpolant of ψ_i over the nodes. In particular, denoting $x_k = kh$ we have

$$\tilde{\psi}_{h,i}(x) = \psi_i(x_k) + \frac{x - x_k}{x_{k+1} - x_k} [\psi_i(x_{k+1}) - \psi_i(x_k)] \quad \text{on } [x_k, x_{k+1}].$$

Taylor expanding at x we have

$$\begin{aligned} \psi_i(x_{k+1}) &= \psi_i(x) + \psi_i'(x)(x_{k+1} - x) + \frac{\psi_i''(\eta_1)}{2}(x_{k+1} - x)^2 & x < \eta_1 < x_{k+1} \\ \psi_i(x_k) &= \psi_i(x) + \psi_i'(x)(x_k - x) + \frac{\psi_i''(\eta_2)}{2}(x_k - x)^2 & x_k < \eta_2 < x. \end{aligned}$$

Therefore

$$\tilde{\psi}_{h,i}(x) = \psi_i(x) + \frac{\psi_i''(\eta_2)}{2}(x_k - x)^2 + \frac{x - x_k}{x_{k+1} - x_k} \left[\frac{\psi_i''(\eta_1)}{2}(x_{k+1} - x)^2 + \frac{\psi_i''(\eta_2)}{2}(x_k - x)^2 \right]$$

and since $\|\psi_i''\|_\infty \leq \lambda_i$ we have

$$\sup_{x \in [x_k, x_{k+1}]} |\tilde{\psi}_{h,i}(x) - \psi_i(x)| \leq C \lambda_i h^2.$$

Therefore $\|\tilde{\psi}_{h,i} - \psi_i\|_\infty \leq C \lambda_i h^2$ and the result follows. \square

Proof of Lemma 3.4. Notice that

$$|\Lambda_{\mathbf{h},\mathbf{i}} - \Lambda_{\mathbf{i}}| \leq \sum_{d=1}^D |\lambda_{h_d, i_d} - \lambda_{i_d}|$$

and

$$\begin{aligned} |\Psi_{\mathbf{h},\mathbf{i}}(\mathbf{x}) - \Psi_{\mathbf{i}}(\mathbf{x})| &= \left| \prod_{d=1}^D \psi_{h_d, i_d}(x_d) - \prod_{d=1}^D \psi_{i_d}(x_d) \right| \\ &\leq \sum_{d=1}^D \left(|\psi_{h_d, i_d}(x_d) - \psi_{i_d}(x_d)| \prod_{\ell=1}^{d-1} |\psi_{i_\ell}(x_\ell)| \prod_{\ell=d+1}^D |\psi_{h_\ell, i_\ell}(x_\ell)| \right). \end{aligned}$$

Therefore the result follows from the one-dimensional estimates in Lemma 3.2. \square

Proof of Lemma 3.6. We shall abuse the notation and order the multi index $\mathbf{i} \in \mathbb{N}^D$ as a single sequence $i \in \mathbb{N}$ so that

$$\begin{aligned} u &= \kappa^{s-D/2} \sum_{i=1}^{\infty} (\kappa^2 + \Lambda_i)^{-\frac{s}{2}} \xi_i \Psi_i, \\ u_{\mathbf{h}} &= \kappa^{s-D/2} \sum_{i=1}^{n_{\mathbf{h}}} (\kappa^2 + \Lambda_{\mathbf{h},i})^{-\frac{s}{2}} \xi_i \Psi_{\mathbf{h},i}. \end{aligned}$$

Bound for $\mathbb{E}\|u_{\mathbf{h}} - u\|_2^2$ This can be proven using the techniques in [3, Theorem 2.10] and in the L^∞ bound that we will establish below.

Hölder continuity We have

$$\begin{aligned} \mathbb{E}|u(\mathbf{x} + \mathbf{h}) - u(\mathbf{x})|^2 &\lesssim \sum_{i=1}^{\infty} (\kappa^2 + \Lambda_i)^{-s} |\Psi_i(\mathbf{x} + \mathbf{h}) - \Psi_i(\mathbf{x})|^2 \\ &\lesssim \sum_{i=1}^{\infty} (\kappa^2 + \Lambda_i)^{-s} \min\{\|\nabla \Psi_i\|_\infty^2 h^2, 1\} \\ &\lesssim \sum_{i=1}^{\infty} i^{-\frac{2s}{D}} \min\{i^{\frac{2}{D}} h^2, 1\} \\ &\lesssim \int_{x \geq 1} x^{-\frac{2s}{D}} \min\{x^{\frac{2}{D}} h^2, 1\} dx \\ &\lesssim \left[\int_{1 \leq x \leq h^{-D}} h^2 x^{-\frac{2}{D} - \frac{2s}{D}} dx + \int_{x > h^{-D}} x^{-\frac{2s}{D}} dx \right] \\ &\lesssim h^{2s-D}, \end{aligned}$$

where we have used that $\|\nabla \Psi_i\|_\infty \leq \sqrt{\Lambda_i}$ and Weyl's law $\Lambda_i \asymp i^{2/D}$. Then by [48, Corollary 6.8] we have

$$\mathbb{E}|u(\mathbf{x}) - u(\mathbf{x}')|^{2p} \leq C_p |\mathbf{x} - \mathbf{x}'|^{(2s-D)p}$$

for all $p \in \mathbb{N}$. Kolmogorov continuity theorem [48, Theorem 6.24] implies that u is β -Hölder for $\beta < \frac{(2s-D)p-2D}{2p}$. Letting $p \rightarrow \infty$ gives the desired result.

Bound for $\mathbb{E}\|u_{\mathbf{h}} - u\|_\infty^2$ Consider two intermediate quantities

$$\tilde{u} = \kappa^{s-D/2} \sum_{i=1}^{n_{\mathbf{h}}} (\kappa^2 + \Lambda_i)^{-\frac{s}{2}} \xi_i \Psi_i, \quad (6.2)$$

$$\tilde{u}_{\mathbf{h}} = \kappa^{s-D/2} \sum_{i=1}^{n_{\mathbf{h}}} (\kappa^2 + \Lambda_i)^{-\frac{s}{2}} \xi_i \Psi_{\mathbf{h},i}. \quad (6.3)$$

We have

$$\begin{aligned} \mathbb{E}\|u - u_{\mathbf{h}}\|_\infty^2 &\leq \mathbb{E}(\|u - \tilde{u}\|_\infty + \|\tilde{u} - \tilde{u}_{\mathbf{h}}\|_\infty + \|\tilde{u}_{\mathbf{h}} - u_{\mathbf{h}}\|_\infty)^2 \\ &\leq 2\left(\mathbb{E}\|u - \tilde{u}\|_\infty^2 + \mathbb{E}\|\tilde{u} - \tilde{u}_{\mathbf{h}}\|_\infty^2 + \mathbb{E}\|\tilde{u}_{\mathbf{h}} - u_{\mathbf{h}}\|_\infty^2\right) \end{aligned}$$

and it suffices to bound each term. Since the Ψ_i 's are uniformly bounded and that ξ has bounded first moment, we have

$$\begin{aligned} \mathbb{E}\|u - \tilde{u}\|_\infty^2 &\leq \kappa^{2s-D} \mathbb{E} \left[\sum_{i=n_{\mathbf{h}}+1}^{\infty} (\kappa^2 + \Lambda_i)^{-\frac{s}{2}} |\xi_i| \|\Psi_i\|_\infty \right]^2 \\ &\lesssim \kappa^{2s-D} \left[\sum_{i=n_{\mathbf{h}}+1}^{\infty} (\kappa^2 + \Lambda_i)^{-\frac{s}{2}} \right]^2 \\ &\lesssim \kappa^{2s-D} \left(\sum_{i=n_{\mathbf{h}}+1}^{\infty} i^{-\frac{s}{D}} \right)^2 \lesssim \kappa^{2s-D} n_{\mathbf{h}}^{2-\frac{2s}{D}} \asymp \kappa^{2s-D} h^{2s-2D}. \end{aligned} \quad (6.4)$$

Similarly, by Lemma 3.4

$$\begin{aligned} \mathbb{E}\|\tilde{u} - \tilde{u}_{\mathbf{h}}\|_\infty^2 &\lesssim \kappa^{2s-D} \left[\sum_{i=1}^{n_{\mathbf{h}}} (\kappa^2 + \Lambda_i)^{-\frac{s}{2}} \|\Psi_i - \Psi_{\mathbf{h},i}\|_\infty \right]^2 \\ &\lesssim \kappa^{2s-D} h^4 \left(\sum_{i=1}^{n_{\mathbf{h}}} \Lambda_i^{1-\frac{s}{2}} \right)^2 \lesssim \kappa^{2s-D} h^4 \left[1 \vee n_{\mathbf{h}}^{2+\frac{4}{d}(1-\frac{s}{2})} \right] \asymp \kappa^{2s-D} h^{(2s-2s)\wedge 4}. \end{aligned} \quad (6.5)$$

For the last term we have by Lemma 3.4

$$\begin{aligned} \mathbb{E}\|\tilde{u}_{\mathbf{h}} - u_{\mathbf{h}}\|_\infty^2 &\lesssim \kappa^{2s-D} \left[\sum_{i=1}^{n_{\mathbf{h}}} \left| (\kappa^2 + \Lambda_i)^{-\frac{s}{2}} - (\kappa^2 + \Lambda_{\mathbf{h},i})^{-\frac{s}{2}} \right| \right]^2 \\ &\lesssim \kappa^{2s-D} \left[\sum_{i=1}^{n_{\mathbf{h}}} \Lambda_i^{-\frac{s}{2}-1} |\Lambda_i - \Lambda_{\mathbf{h},i}| \right]^2 \lesssim \kappa^{2s-D} h^4 \left(\sum_{i=1}^{n_{\mathbf{h}}} \Lambda_i^{1-\frac{s}{2}} \right)^2 \lesssim \kappa^{2s-D} h^{(2s-2d)\wedge 4}. \end{aligned} \quad (6.6)$$

The result follows by combining (6.4), (6.5), (6.6). \square

Proof of Proposition 3.11. Again we shall abuse the notation and write

$$u = \kappa^{s-D/2} \sum_{i=1}^{\infty} (\kappa^2 + \Lambda_i)^{-s/2} \xi_i \Psi_i.$$

L^∞ case Recall that

$$\varphi_{f_0}(\varepsilon; u, \|\cdot\|_\infty) = \inf_{g \in \mathbb{H}: \|g - f_0\|_\infty < \varepsilon} \|g\|_{\mathbb{H}}^2 - \log \mathbb{P}(\|u\|_\infty < \varepsilon).$$

By [27, Theorem 1.2], the second term can be bounded by analyzing the $L^\infty(\mathcal{D})$ metric entropy of \mathbb{H}_1 , the unit ball of \mathbb{H} . Notice that \mathbb{H}_1 takes the form

$$\mathbb{H}_1 = \left\{ \sum_{i=1}^{\infty} g_i \Psi_i : \sum_{i=1}^{\infty} g_i^2 (\kappa^2 + \Lambda_i)^s \leq 1 \right\}$$

and is contained in a Sobolev ball of order s , whose $L^\infty(\mathcal{D})$ metric entropy is bounded by a constant times $\varepsilon^{-\frac{D}{s}}$ (see e.g. [13, Theorem 3.3.2]). Then [27, Theorem 1.2] implies that

$$-\log \mathbb{P}(\|u\|_\infty < \varepsilon) \lesssim \varepsilon^{-\frac{2D}{2s-D}} = \varepsilon^{-\frac{D}{\beta}}, \quad (6.7)$$

where we used the assumption that $s = \beta + \frac{D}{2}$. For the first term, let $C_0 = \|f_0\|_{B_{\infty,\infty}^\beta}$ and consider $g = S_J(\sqrt{\Delta})f_0$ with J the smallest integer such that $C_0 2^{-\beta J} < \varepsilon$. Since $f_0 \in B_{\infty,\infty}^\beta$ we have

$$\|S_j(\sqrt{\Delta})f_0 - f_0\|_\infty \leq C_0 2^{-\beta j} \quad (6.8)$$

for all j . In particular, $\|g - f_0\|_\infty \leq C_0 2^{-\beta J} \leq \varepsilon$. Moreover we have $g = \sum_{i=1}^{\infty} S_J(\sqrt{\Lambda_i})f_i \Psi_i$ as a finite series since $S_J(\sqrt{\Lambda_i}) = 0$ if $\sqrt{\Lambda_i} > 2^J$ and hence $g \in \mathbb{H}$. Now since $S_j \leq 1$,

$$\|g\|_{\mathbb{H}}^2 \leq \sum_{\sqrt{\Lambda_i} \leq 2^J} f_i^2 (\kappa^2 + \Lambda_i)^s = \sum_{\sqrt{\Lambda_i} \leq 1} f_i^2 (\kappa^2 + \Lambda_i)^s + \sum_{j=1}^J \sum_{2^{j-1} < \sqrt{\Lambda_i} \leq 2^j} f_i^2 (\kappa^2 + \Lambda_i)^s.$$

By (6.8) we have

$$\begin{aligned} \sum_{2^{j-1} < \sqrt{\Lambda_i} \leq 2^j} f_i^2 (\kappa^2 + \Lambda_i)^s &\lesssim 2^{2js} \sum_{2^{j-1} < \sqrt{\Lambda_i}} f_i^2 \lesssim 2^{2js} \|S_j(\sqrt{\Delta})f_0 - f_0\|_\infty^2 \\ &\lesssim 2^{2js} \|S_j(\sqrt{\Delta})f_0 - f_0\|_\infty^2 \lesssim 2^{2(s-\beta)j}. \end{aligned}$$

Since J is the smallest integer such that $C_0 2^{-\beta J} < \varepsilon$, we have $2^{-\beta J} \gtrsim \varepsilon$ and hence

$$\|g\|_{\mathbb{H}}^2 \lesssim \sum_{\sqrt{\Lambda_i} \leq 1} f_i^2 + \sum_{j=1}^J 2^{2(s-\beta)j} \lesssim 2^{2(s-\beta)J} \lesssim \varepsilon^{-\frac{2(s-\beta)}{\beta}} = \varepsilon^{-\frac{D}{\beta}}. \quad (6.9)$$

Combining (6.7) and (6.9) we deduce that

$$\varphi_{f_0}(\varepsilon) \lesssim \varepsilon^{-\frac{D}{\beta}}$$

and setting $\varepsilon_n = Cn^{-\frac{\beta}{2\beta+D}}$ for a large enough constant C gives the result.

L^2 case We have

$$\varphi_{f_0}(\varepsilon; u, \|\cdot\|_2) = \inf_{g \in \mathbb{H}: \|g - f_0\|_2 < \varepsilon} \|g\|_{\mathbb{H}}^2 - \log \mathbb{P}(\|u\|_2 < \varepsilon). \quad (6.10)$$

For the second term, recall that $u = \kappa^{s-D/2} \sum_{i=1}^{\infty} (\kappa^2 + \Lambda_i)^{-s/2} \xi_i \Psi_i$. We then have

$$\begin{aligned} \log \mathbb{P}(\|u\|_2 < \varepsilon) &= \log \mathbb{P}\left(\kappa^{2s-D} \sum_{i=1}^{\infty} (\kappa^2 + \Lambda_i)^{-s} \xi_i^2 < \varepsilon\right) \\ &\geq \log \mathbb{P}\left(\sum_{i=1}^{\infty} i^{-\frac{2s}{D}} \xi_i^2 < C\varepsilon\right) \gtrsim \varepsilon^{-\frac{2}{\frac{2s}{D}-1}} = \varepsilon^{-\frac{D}{\beta}}, \end{aligned} \quad (6.11)$$

where the last step follows from [12, Corollary 6] and the assumption that $s = \beta + \frac{D}{2}$. For the first term in (6.10), let $C_0 = \|f_0\|_{B_{\infty,\infty}^{\beta}}$ and consider $g = S_J(\sqrt{\Delta})f_0$ with J the smallest integer so that $C_0\sqrt{|\mathcal{D}|}2^{-\beta J} < \varepsilon$, where $|\mathcal{D}|$ is the Lebesgue measure of \mathcal{D} . Since $f_0 \in B_{\infty,\infty}^{\beta}$ we have

$$\|S_j(\sqrt{\Delta})f_0 - f_0\|_{\infty} \leq C_0 2^{-\beta j}$$

for all j . In particular, $\|g - S_J(\sqrt{\Delta})f_0\|_2 \leq \sqrt{|\mathcal{D}|} \|g - S_J(\sqrt{\Delta})f_0\|_{\infty} \leq C_0\sqrt{|\mathcal{D}|}2^{-\beta J} \leq \varepsilon$. Now proceeding in the same way as the argument in the L^{∞} case we obtain

$$\|g\|_{\mathbb{H}}^2 \lesssim \sum_{\sqrt{\lambda_i} \leq 1} f_i^2 + \sum_{j=1}^J 2^{2(s-\beta)j} \lesssim 2^{2(s-\beta)J} \lesssim \varepsilon^{-\frac{2(s-\beta)}{\beta}} = \varepsilon^{-\frac{D}{\beta}}, \quad (6.12)$$

where we have used the fact that $2^{-\beta J} \gtrsim \varepsilon$ since J is the smallest integer such that $C_0\sqrt{|\mathcal{D}|}2^{-\beta J} < \varepsilon$. Combining (6.11) and (6.12) we deduce that

$$\varphi_{f_0}(\varepsilon) \lesssim \varepsilon^{-\frac{D}{\beta}},$$

and setting $\varepsilon_n = Cn^{-\frac{\beta}{2\beta+D}}$ for a large enough constant C gives the result. \square

Acknowledgements

Both authors are thankful for the support of NSF and NGA through the grant DMS-2027056. DSA is also supported by a Fundaci3n BBVA start-up grant. The authors are grateful to Ridgway Scott for helpful discussions.

References

- [1] D. Bolin and K. Kirchner. The rational SPDE approach for Gaussian random fields with general smoothness. *Journal of Computational and Graphical Statistics*, 29(2):274–285, 2020.
- [2] D. Bolin and F. Lindgren. A comparison between Markov approximations and other methods for large spatial data sets. *Computational Statistics & Data Analysis*, 61:7–21, 2013.
- [3] D. Bolin, K. Kirchner, and M. Kovács. Numerical solution of fractional elliptic stochastic PDEs with spatial white noise. *IMA Journal of Numerical Analysis*, 40(2):1051–1073, 2020.

- [4] M. Cameletti, F. Lindgren, D. Simpson, and H. Rue. Spatio-temporal modeling of particulate matter concentration through the SPDE approach. *AStA Advances in Statistical Analysis*, 97(2):109–131, 2013.
- [5] I. Castillo, G. Kerkyacharian, and D. Picard. Thomas Bayes’ walk on manifolds. *Probability Theory and Related Fields*, 158(3):665–710, 2014.
- [6] S. Cotter, M. Dashti, and A. M. Stuart. MCMC methods for functions: modifying old algorithms to make them faster. *SIAM Journal on Numerical Analysis*, 48(1):322–345, 2010.
- [7] S. G. Cox and K. Kirchner. Regularity and convergence analysis in Sobolev and Hölder spaces for generalized Whittle–Matérn fields. *Numerische Mathematik*, 146(4):819–873, 2020.
- [8] T. Cui, K. J. Law, and Y. M. Marzouk. Dimension-independent likelihood-informed MCMC. *Journal of Computational Physics*, 304:109–137, 2016.
- [9] A. Datta, S. Banerjee, A. O. Finley, and A. E. Gelfand. Hierarchical nearest-neighbor Gaussian process models for large geostatistical datasets. *Journal of the American Statistical Association*, 111(514):800–812, 2016.
- [10] E. B. Davies. *Spectral Theory and Differential Operators*. Number 42. Cambridge University Press, 1996.
- [11] J. Du, H. Zhang, and V. Mandrekar. Fixed-domain asymptotic properties of tapered maximum likelihood estimators. *The Annals of Statistics*, 37(6A):3330–3361, 2009.
- [12] T. Dunker, M. Lifshits, and W. Linde. Small deviation probabilities of sums of independent random variables. In *High Dimensional Probability*, pages 59–74. Springer, 1998.
- [13] D. E. Edmunds and H. Triebel. *Function Spaces, Entropy Numbers, Differential Operators*, volume 120. Cambridge University Press Cambridge, 1996.
- [14] R. Furrer, M. G. Genton, and D. Nychka. Covariance tapering for interpolation of large spatial datasets. *Journal of Computational and Graphical Statistics*, 15(3):502–523, 2006.
- [15] N. Garcia Trillos, Z. Kaplan, T. Samakhoana, and D. Sanz-Alonso. On the consistency of graph-based Bayesian semi-supervised learning and the scalability of sampling algorithms. *Journal of Machine Learning Research*, 21(28):1–47, 2020.
- [16] G. Gaspari and S. E. Cohn. Construction of correlation functions in two and three dimensions. *Quarterly Journal of the Royal Meteorological Society*, 125(554):723–757, 1999.
- [17] A. E. Gelfand, P. Diggle, P. Guttorp, and M. Fuentes. *Handbook of Spatial Statistics*. CRC press, 2010.
- [18] S. Ghosal, J. K. Ghosh, and A. Van Der Vaart. Convergence rates of posterior distributions. *The Annals of Statistics*, pages 500–531, 2000.
- [19] M. Giordano and R. Nickl. Consistency of Bayesian inference with Gaussian process priors in an elliptic inverse problem. *Inverse Problems*, 36(8):085001, 2020.

- [20] P. Greengard and M. O’Neil. Efficient reduced-rank methods for Gaussian processes with eigenfunction expansions. *arXiv preprint arXiv:2108.05924*, 2021.
- [21] P. Guttorp and T. Gneiting. Studies in the history of probability and statistics XLIX: On the Matérn correlation family. *Biometrika*, 93(4):989–995, 2006.
- [22] M. J. Heaton, A. Datta, A. O. Finley, R. Furrer, J. Guinness, F. Guhaniyogi, R. and Gerber, R. B. Gramacy, D. Hammerling, M. Katzfuss, et al. A case study competition among methods for analyzing large spatial data. *Journal of Agricultural, Biological and Environmental Statistics*, 24(3):398–425, 2019.
- [23] P. L. Houtekamer and H. L. Mitchell. A sequential ensemble Kalman filter for atmospheric data assimilation. *Monthly Weather Review*, 129(1):123–137, 2001.
- [24] M. Kang and M. Katzfuss. Correlation-based sparse inverse Cholesky factorization for fast Gaussian-process inference. *arXiv preprint arXiv:2112.14591*, 2021.
- [25] M. Katzfuss and J. Guinness. A general framework for Vecchia approximations of Gaussian processes. *Statistical Science*, 36(1):124–141, 2021.
- [26] U. Khristenko, L. Scarabosio, P. Swierczynski, E. Ullmann, and B. Wohlmuth. Analysis of boundary effects on PDE-based sampling of Whittle–Matérn random fields. *SIAM/ASA Journal on Uncertainty Quantification*, 7(3):948–974, 2019.
- [27] W. V. Li and W. Linde. Approximation, metric entropy and small ball estimates for Gaussian measures. *The Annals of Probability*, 27(3):1556–1578, 1999.
- [28] F. Lindgren, H. Rue, and J. Lindström. An explicit link between Gaussian fields and Gaussian Markov random fields: the stochastic partial differential equation approach. *Journal of the Royal Statistical Society: Series B (Statistical Methodology)*, 73(4):423–498, 2011.
- [29] F. Lindgren, D. Bolin, and H. Rue. The SPDE approach for Gaussian and non-Gaussian fields: 10 years and still running. *Spatial Statistics*, page 100599, 2022.
- [30] R. Neal. Regression and classification using Gaussian process priors. *Bayesian Statistics*, 6, 1998.
- [31] R. Nickl, S. van de Geer, and S. Wang. Convergence rates for penalized least squares estimators in PDE constrained regression problems. *SIAM/ASA Journal on Uncertainty Quantification*, 8(1):374–413, 2020.
- [32] H. Owhadi and C. Scovel. *Operator-Adapted Wavelets, Fast Solvers, and Numerical Homogenization: From a Game Theoretic Approach to Numerical Approximation and Algorithm Design*, volume 35. Cambridge University Press, 2019.
- [33] H. Owhadi, C. Scovel, and F. Schäfer. Statistical numerical approximation. *Notices of the American Mathematical Society*, 66:1608–1617, 2019.

- [34] J. Quinero-Candela and C. E. Rasmussen. A unifying view of sparse approximate Gaussian process regression. *Journal of Machine Learning Research*, 6:1939–1959, 2005.
- [35] H. Rue and L. Held. *Gaussian Markov Random Fields: Theory and Applications*. Chapman and Hall/CRC, 2005.
- [36] D. Sanz-Alonso and R. Yang. The SPDE approach to Matérn fields: Graph representations. *To appear in Statistical Science*, 2022.
- [37] D. Sanz-Alonso and R. Yang. Unlabeled data help in graph-based semi-supervised learning: A Bayesian nonparametrics perspective. *To appear in Journal of Machine Learning Research*, 2022.
- [38] D. Sanz-Alonso, A. M. Stuart, and A. Taeb. Inverse Problems and Data Assimilation. *arXiv preprint arXiv:1810.06191*, 2019.
- [39] F. Schäfer, M. Katzfuss, and H. Owhadi. Sparse Cholesky factorization by Kullback–Leibler minimization. *SIAM Journal on Scientific Computing*, 43(3):A2019–A2046, 2021.
- [40] A. Solin and S. Särkkä. Hilbert space methods for reduced-rank Gaussian process regression. *Statistics and Computing*, 30(2):419–446, 2020.
- [41] M. L. Stein. Bounds on the efficiency of linear predictions using an incorrect covariance function. *The Annals of Statistics*, pages 1116–1138, 1990.
- [42] M. L. Stein. Uniform asymptotic optimality of linear predictions of a random field using an incorrect second-order structure. *The Annals of Statistics*, pages 850–872, 1990.
- [43] M. L. Stein. A simple condition for asymptotic optimality of linear predictions of random fields. *Statistics & Probability Letters*, 17(5):399–404, 1993.
- [44] M. L. Stein. *Interpolation of Spatial Data: Some Theory for Kriging*. Springer Science & Business Media, 1999.
- [45] M. L. Stein. Predicting random fields with increasing dense observations. *The Annals of Applied Probability*, 9(1):242–273, 1999.
- [46] M. L. Stein. The screening effect in kriging. *The Annals of Statistics*, 30(1):298–323, 2002.
- [47] G. Strang and G. J. Fix. *An Analysis of the Finite Element Method*. Englewood Cliffs, N. J., Prentice-Hall, Inc., 1973. 318 p, 1973.
- [48] A. M. Stuart. Inverse problems: a Bayesian perspective. *Acta Numerica*, 19:451–559, 2010.
- [49] T. J. Sullivan. *Introduction to Uncertainty Quantification*, volume 63. Springer, 2015.
- [50] A. van der Vaart and H. van Zanten. Rates of contraction of posterior distributions based on Gaussian process priors. *The Annals of Statistics*, 36(3):1435–1463, 2008.

- [51] A. van der Vaart and H. van Zanten. Reproducing kernel Hilbert spaces of Gaussian priors. In *Pushing the limits of contemporary statistics: contributions in honor of Jayanta K. Ghosh*, pages 200–222. Institute of Mathematical Statistics, 2008.
- [52] A. van der Vaart and H. van Zanten. Information rates of nonparametric Gaussian process methods. *Journal of Machine Learning Research*, 12(60):2095–2119, 2011.
- [53] A. V. Vecchia. Estimation and model identification for continuous spatial processes. *Journal of the Royal Statistical Society: Series B (Statistical Methodology)*, 50(2):297–312, 1988.
- [54] D. Wang and W.-L. Loh. On fixed-domain asymptotics and covariance tapering in Gaussian random field models. *Electronic Journal of Statistics*, 5:238–269, 2011.
- [55] P. Whittle. On stationary processes in the plane. *Biometrika*, pages 434–449, 1954.
- [56] C. K. I. Williams and C. E. Rasmussen. *Gaussian Processes for Machine Learning*, volume 2. MIT press Cambridge, MA, 2006.